Supplementary Information

Visible-Light-Driven Photocontrol of the Trp-cage Protein Fold by a Diazocine Cross-Linker

Nils Preußke, Widukind Moormann, Katrin Bamberg, Matthias Lipfert, Rainer Herges, Frank D. Sönnichsen

Otto Diels-Institute for Organic Chemistry, Christian-Albrechts-University of Kiel, 24119 Kiel, Germany

Contents

1. Distance Computation

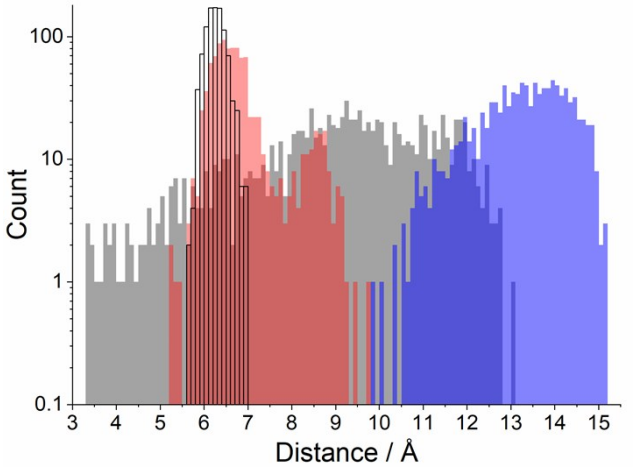

Fig. S 1: The same computed distances of the switchable Trp-cage 'cis-SC_a' (open), the uncross-linked Trp-cage 'TC(4,8)' (red), as well as the diazocines *cis*-**5** (gray) and *trans*-**5** (blue) as in **Fig. 3** (in the paper) are here displayed on a logarithmic scale.

2. Characterization of TC(4,8)

2.1. UHPLC-HRMS

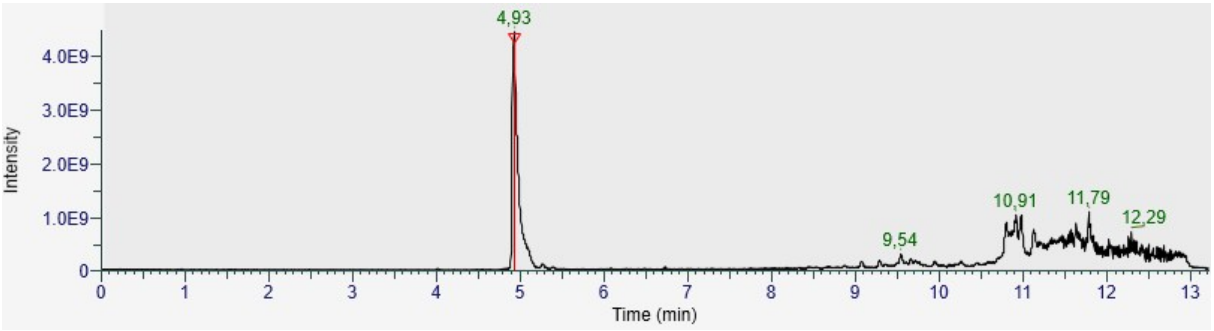

Fig. S 2: Chromatogram of TC(4,8). Peaks after 9 min are background noise.

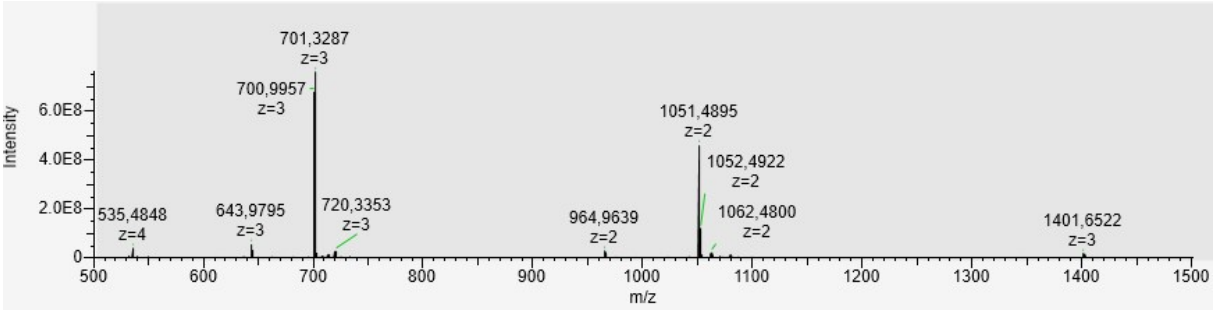

Fig. S 3: Mass spectrum of TC(4,8) at a retention time of 4.93 min. The peaks at 535, 701 and 1051 result from different charged states of TC(4,8). The small peaks immediately to the right of peak 701 and peak 1051 correspond to adducts of TC(4,8) with Na^+ and/or K^+. The peak at 1402 corresponds to the non-covalent homodimer of TC(4,8) $[2M + 3H]^{3+}$. The peaks at 644 and 965 belong to a side product from solid phase synthesis of TC(4,8) that possesses a similar retention time as TC(4,8). Based on the MS-detected chromatogram the sample is at least 80% pure.

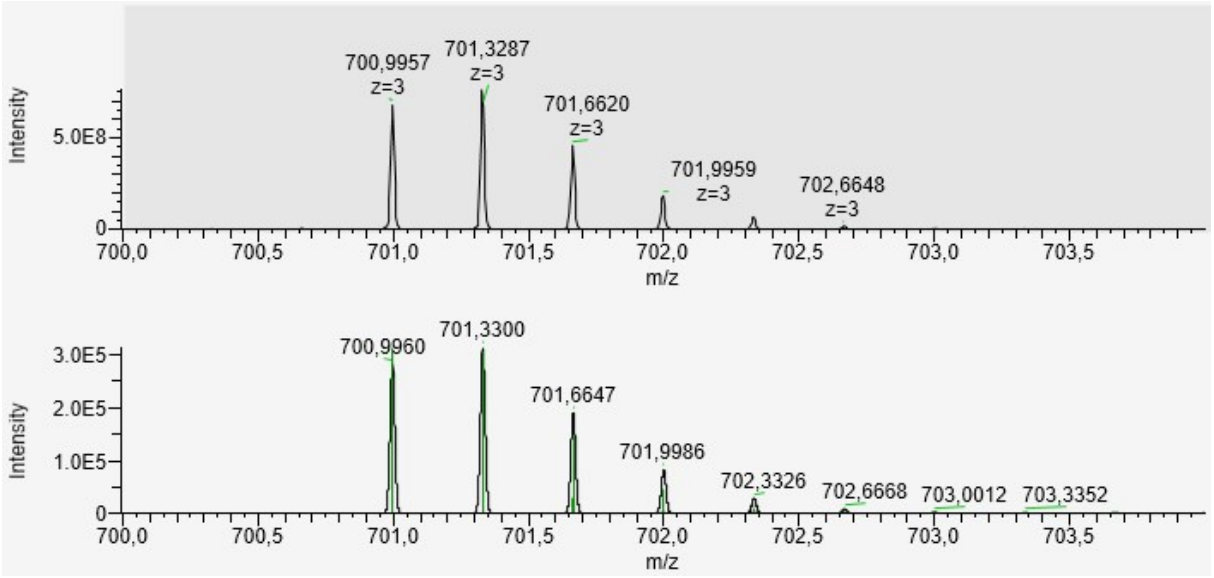

Fig. S 4: The expansion of the mass spectrum in **Fig. S 3** in the range between 700 and 704 demonstrates that the isotopic pattern of TC(4,8) (top) is identical with the isotopic pattern calculated based on its sum formula $[C_{91}H_{133}N_{27}O_{31} + 3H]^{3+}$ (bottom).

2.2. NMR data

Tab. S 1: Proton chemical shifts of the folded main form of TC(4,8).

No.	Res.	Proton: Shift / ppm
00	Ac	Me: 2.074
01	D	H^{N}: 8.245, H^{α}: 4.565, $H^{\beta 2/\beta 3}$: 2.828/2.726
02	A	H^{N}: 8.658, H^{α}: 4.185, H^{β}: 1.389
03	Y	H^{N}: 8.771, H^{α}: 4.248, H^{β}: 3.093, H^{δ}: 7.098, H^{ϵ}: 6.832
04	Γ	H^{N}: 8.622, H^{α}: 4.473, H^{β}: 3.470
05	Q	H^{N}: 8.465, H^{α}: 4.019, H^{β}: 2.114, H^{γ}: 2.311, $H^{\epsilon 21/\epsilon 22}$: 7.618/6.870
06	W	H^{N}: 8.228, H^{α}: 4.396, $H^{\beta 2/\beta 3}$: 3.394/3.204, $H^{\delta 1}$: 7.091, $H^{\epsilon 1}$: 9.873, $H^{\zeta 2}$: 7.308, $H^{\eta 2}$: 7.221, $H^{\epsilon 3}$: 7.135, $H^{\zeta 3}$: 7.226
07	L	H^{N}: 8.415, H^{α}: 3.696, $H^{\beta 2/\beta 3}$: 1.721/1.472, H^{γ}: 1.547, $H^{\delta 1/\delta 2}$: 0.937/0.854
08	Γ	H^{N}: 8.276, H^{α}: 4.467, $H^{\beta 2/\beta 3}$: 3.490/3.418
09	D	H^{N}: 8.055, H^{α}: 4.628, $H^{\beta 2/\beta 3}$: 2.840/2.699
10	G	H^{N}: 7.773, $H^{\alpha 2/\alpha 3}$: 4.100/3.657
11	G	H^{N}: 8.201, $H^{\alpha 2/\alpha 3}$: 3.420/1.983
12	P	H^{α}: 4.551, $H^{\beta 2/\beta 3}$: 2.440/2.040, H^{γ}: 2.102, $H^{\delta 2/\delta 3}$: 3.740/3.471
13	S	H^{N}: 7.963, H^{α}: 4.468, H^{β}: 3.906
14	S	H^{N}: 8.207, H^{α}: 4.260, $H^{\beta 2/\beta 3}$: 3.885/3.635
15	G	H^{N}: 8.071, $H^{\alpha 2/\alpha 3}$: 4.163/3.861
16	R	H^{N}: 8.096, H^{α}: 4.878, H^{β}: 1.819, $H^{\gamma 2/\gamma 3}$: 1.727/1.657, H^{δ}: 3.228, H^{ϵ}: 7.425
17	P	H^{α}: 4.708, $H^{\beta 2/\beta 3}$: 2.317/1.816, H^{γ}: 1.997, $H^{\delta 2/\delta 3}$: 3.837/3.634
18	P	H^{α}: 3.254, $H^{\beta 2/\beta 3}$: 1.547/1.046, H^{γ}: 1.816, $H^{\delta 2/\delta 3}$: 3.602/3.531
19	P	H^{α}: 4.376, $H^{\beta 2/\beta 3}$: 2.228/1.984, H^{γ}: 1.890, $H^{\delta 2/\delta 3}$: 3.369/3.180
20	S	H^{N}: 7.871, H^{α}: 4.191, H^{β}: 3.801

Assignments are according to IUPAC nomenclature.[1]

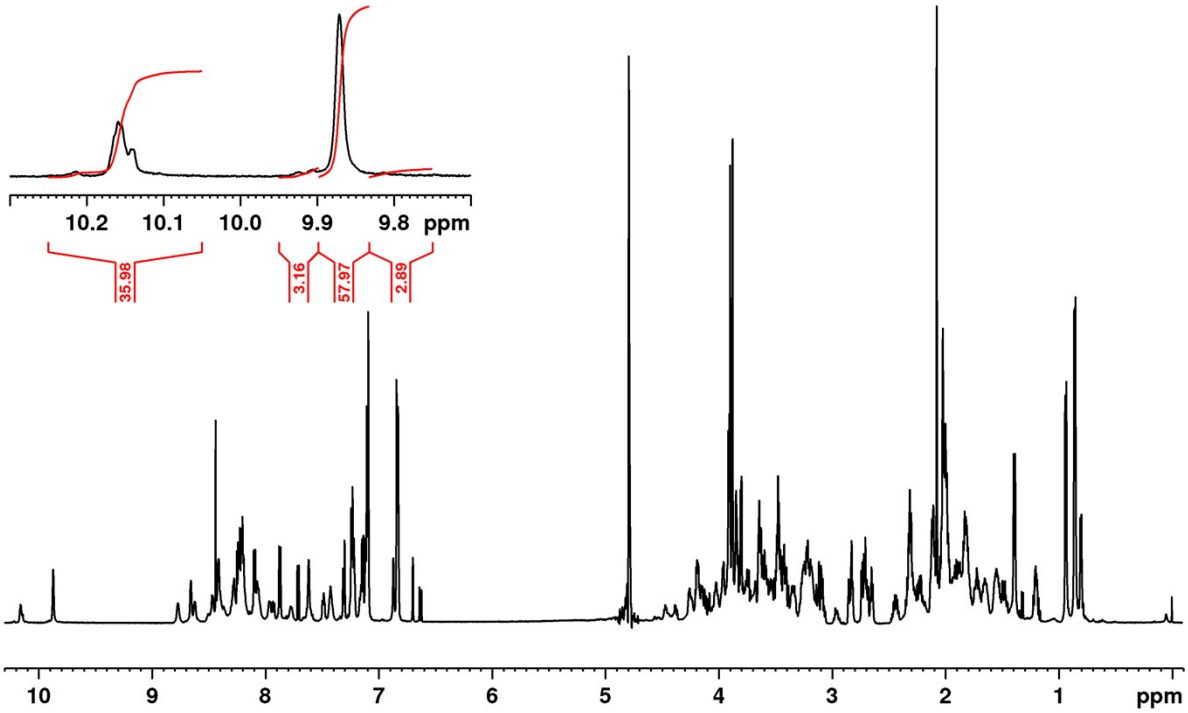

Fig. S 5: 1D ^{1}H-NMR spectrum of TC(4,8) in water with 10% D_2O at pH = 5.3, 298 K and a concentration of 1.6 mM. The expansion between 10.3 ppm and 9.7 ppm highlights the indole region. The highest peak (9.873 ppm) belongs to the Trp6 indole proton ($H^{\varepsilon 1}$) of the folded main form. Additional peaks in the indole region indicate unfolded by-forms of the Trp-cage with chemical shifts of the Trp6 indole proton ($H^{\varepsilon 1}$) around 10.15 ppm.

2.2.1. Trp-cage by-forms

Apart from the folded main-form described above, several by-forms of the Trp-cage are apparent in the indole NH-region in the ^{1}H-NMR spectrum (resonances between 9.7 ppm and 10.3 ppm). These by-forms belong to TC(4,8). They make up approximately 36% of the sample as determined by integration of the indole region (**Fig. S 5**) while ultra-high performance liquid chromatography coupled to high resolution mass spectrometry (UHPLC-HRMS) determined the amount of impurities of the sample to be <20% (**Fig. S 2** and **Fig. S 3**). These unfolded by-forms are detectable in NMR spectroscopy as separate resonances, because they are in slow equilibrium with the folded main population on the NMR chemical shift time scale.

In this paper, all NMR-based evaluations refer to the folded main population if not stated otherwise. In contrast, CD spectroscopy is averaged over every structure (including the folded and unfolded by-forms) weighted with respect to their population

2.3. Determination of midpoint of thermal unfolding of TC(4,8)

Fig 4a (in the paper) displays data of thermal unfolding of TC(4,8) (red triangles). The following function was fitted to the data

$$y = A_2 + \frac{A_1 - A_2}{1 + exp(\frac{x - x_0}{dx})}$$

yielding the following values: A_1 = -13585.51999 ± 850.58255
A_2 = -3298.40652 ± 135.41215
x_0 = 31.62031 ± 2.69452 (in this case $x_0 = T_m$)
dx = 13.99868 ± 1.57008

3. Characterization of the folded *cis*-switch-cage

3.1. UHPLC-HRMS

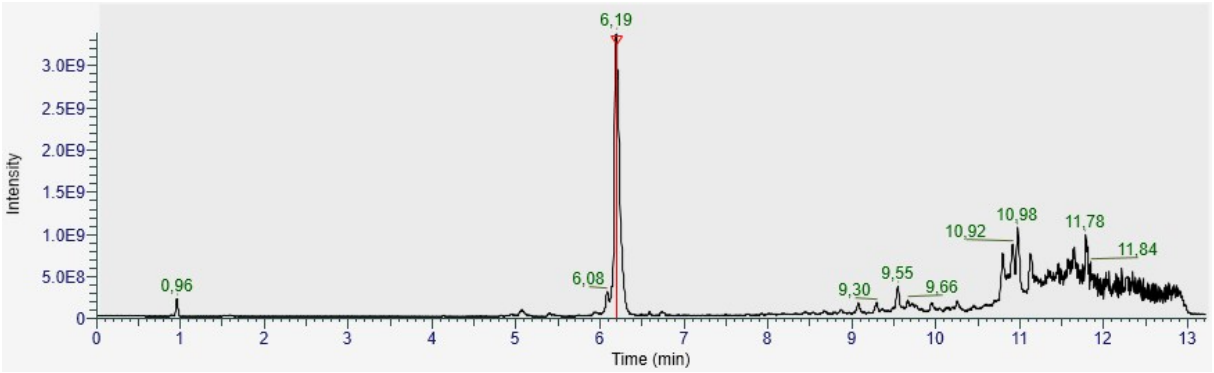

Fig. S 6: Chromatogram of the switch cage. An aliquot of the NMR sample (contains 10% D_2O) was subjected to UHPLC-HRMS analysis. Peaks after 9 min are background noise.

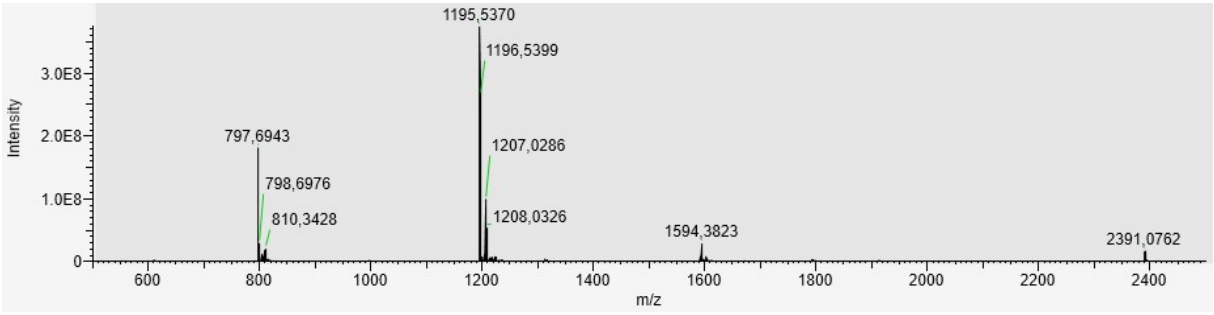

Fig. S 7: Mass spectrum of the switch cage at a retention time of 6.19 min. The peaks around 798, 1196 and 2391 result from different charged states of TC(4,8). The smaller peaks to the right of the product peaks correspond to adducts of the switch cage with Na^+ and/or K^+. The peak around 2391 can be assigned to singly charged switch cage $[M + H]^+$ overlaid the doubly charged non-covalent homodimer of the switch cage $[2M + 2H]^{2+}$. The peak around 1594 belongs to the triply charged non-covalent homodimer $[2M + 3H]^{3+}$. Based on the MS-detected chromatogram the sample is at least 85% pure.

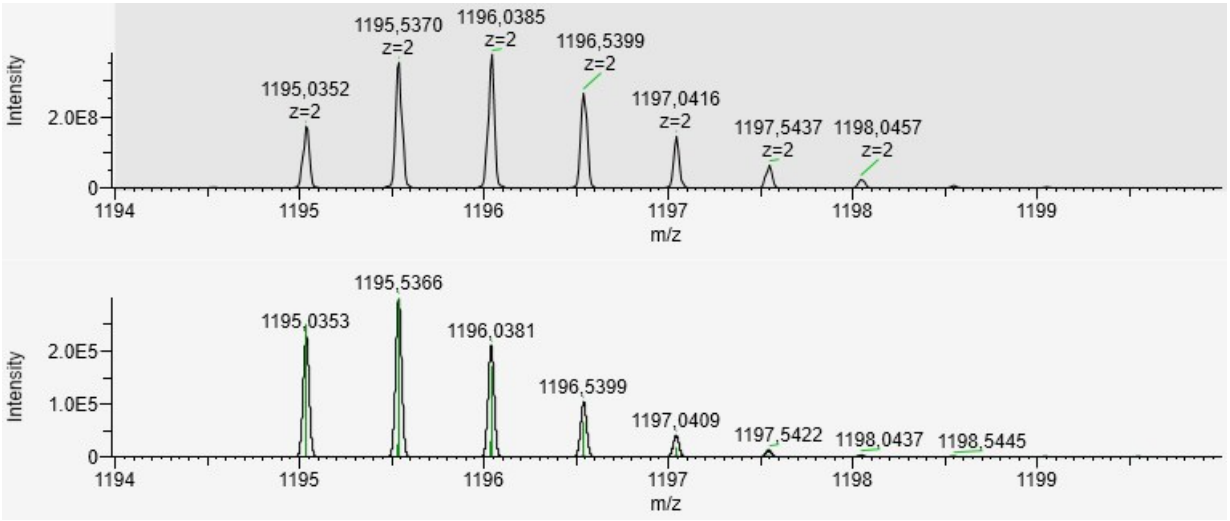

Fig. S 8: The expansion of the mass spectrum in **Fig. S 7** in the range between 1194 and 1200 demonstrates that the isotopic pattern of the switch cage (top) is almost identical with the isotopic pattern calculated based on its sum formula $[C_{109}H_{145}N_{29}O_{33} + 2H]^{2+}$ (bottom). The slight deviation is a result of exchanged protons for deuterons due to the D_2O content of the solvent (cf. **Fig. S 9**).

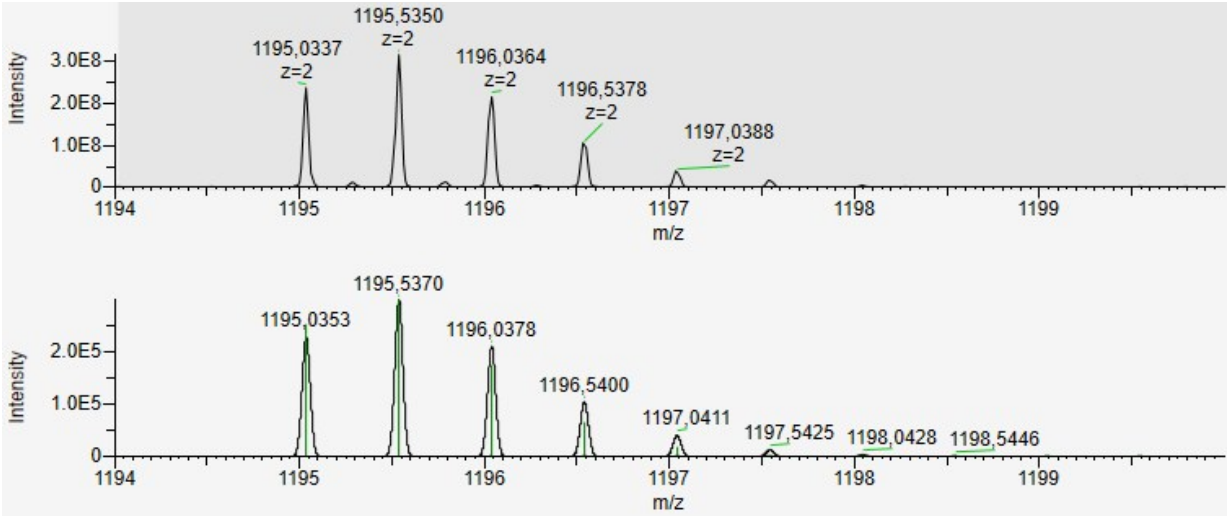

Fig. S 9: The sample from **Fig. S 6**, **Fig. S 7** and **Fig. S 8** was lyophilized and reconstituted with H_2O to exchange all deuterons in the protein with protons. The resulting isotopic pattern of the $[M + 2H]^{2+}$ species exactly matches the predicted pattern. The small peaks in between the isotopic pattern of $[M + 2H]^{2+}$ correspond to the non-covalent homodimer $[2M + 4H]^{4+}$.

3.2. NMR data

3.2.1. Chemical shifts

Tab. S 2: Proton chemical shifts of *cis*-SC$_a$.

No.	Res.	Proton: shift / ppm
00	Ac	Me: 2.060
01	D	H^N: 8.236, H^α: 4.622, $H^{\beta2/\beta3}$: 2.881/2.714
02	A	H^N: 8.688, H^α: 4.201, H^β: 1.483
03	Y	H^N: 8.709, H^α: 4.156, $H^{\beta2/\beta3}$: 3.203/3.128, H^δ: 7.118, H^ε: 6.888
04	Γ	H^N: 8.446, H^α: 3.543, H^β: 3.543, H^γ: 7.506, $H^{\varepsilon2/\varepsilon3}$: 3.654/3.418, H^2: 6.714, $H^{4,5}$: 7.030, H^{br}: 2.83 ± 0.07
05	Q	H^N: 8.353, H^α: 3.923, H^β: 2.173, H^γ: 2.360, $H^{\varepsilon21/\varepsilon22}$: 7.693/6.867
06	W	H^N: 8.004, H^α: 4.238, $H^{\beta2/\beta3}$: 3.501/3.195, $H^{\delta1}$: 7.009, $H^{\varepsilon1}$: 9.728, $H^{\zeta2}$: 7.229, $H^{\eta2}$: 7.153, $H^{\varepsilon3}$: 7.063, $H^{\zeta3}$: 7.148
07	L	H^N: 8.487, H^α: 3.414, $H^{\beta2/\beta3}$: 1.724/1.335, H^γ: 1.525, $H^{\delta1/\delta2}$: 0.853/0.655
08	Γ	H^N: 8.252, H^α: 4.412, $H^{\beta2/\beta3}$: 3.960/3.403, H^γ: 7.917, $H^{\varepsilon2/\varepsilon3}$: 3.488/3.400, H^2: 6.662, H^4: 6.442, H^5: 6.942, H^{br}: 2.83 ± 0.07
09	D	H^N: 7.871, H^α: 4.624, $H^{\beta2/\beta3}$: 2.892/2.683
10	G	H^N: 7.484, $H^{\alpha2/\alpha3}$: 4.148/3.497
11	G	H^N: 8.295, $H^{\alpha2/\alpha3}$: 3.123/0.969
12	P	H^α: 4.594, $H^{\beta2/\beta3}$: 2.516/2.069, H^γ: 2.144, $H^{\delta2/\delta3}$: 3.799/3.416
13	S	H^N: 7.698, H^α: 4.474, H^β: 3.920
14	S	H^N: 8.185, H^α: 4.166, $H^{\beta2/\beta3}$: 3.869/3.528
15	G	H^N: 7.926, $H^{\alpha2/\alpha3}$: 4.270/3.812
16	R	H^N: 8.138, H^α: 5.019, $H^{\beta2/\beta3}$: 1.888/1.818, H^γ: 1.658, H^δ: 3.269, H^ε: 7.563
17	P	H^α: 4.748, $H^{\beta2/\beta3}$: 2.339/1.798, H^γ: 2.000, $H^{\delta2/\delta3}$: 3.866/3.672
18	P	H^α: 2.580, $H^{\beta2/\beta3}$: 1.351/0.385, $H^{\gamma2/\gamma3}$: 1.736/1.651, H^δ: 3.519
19	P	H^α: 4.331, $H^{\beta2/\beta3}$: 2.199/1.981, H^γ: 1.857, $H^{\delta2/\delta3}$: 3.163/2.992
20	S	H^N: 7.819, H^α: 4.164, H^β: 3.775

The assignments are according to IUPAC nomenclature.[1] The nomenclature of the cross-linker assignments is shown in **Fig. S 10**.

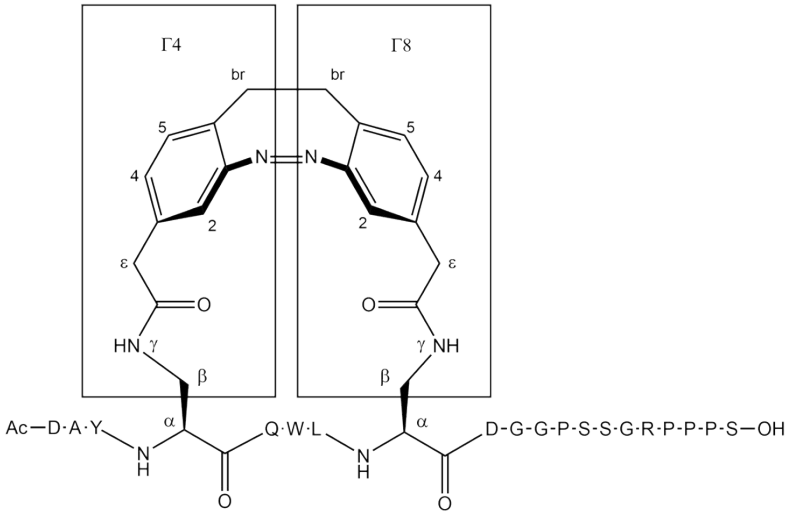

Fig. S 10: The nomenclature of the cross-linker assignments.

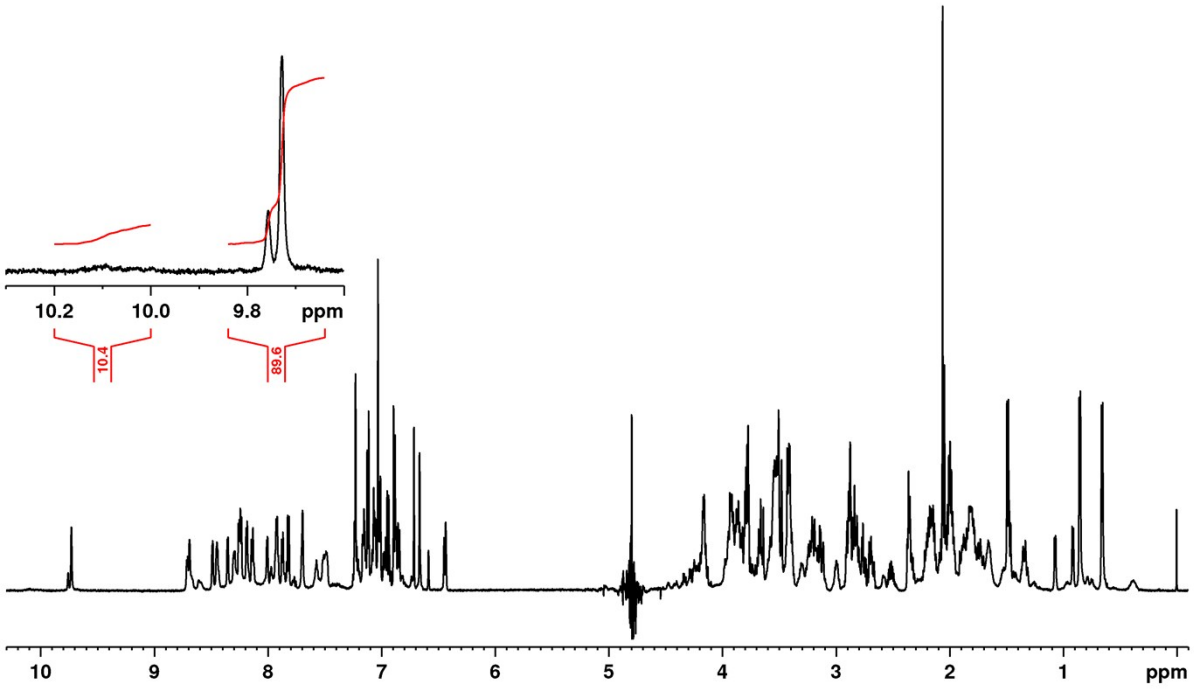

Fig. S 11: 1D ^{1}H-NMR spectrum of the dark-adapted switch cage in water with 10% D_2O at pH = 5.5, 298 K and a concentration of 0.5 mM. The expansion of the region between 10.3 ppm and 9.6 ppm shows that the amount of unfolded by-forms with chemical shifts of the Trp6 indole proton ($H^{\varepsilon 1}$) around 10.1 ppm adds up to approximately 10%, which is significantly reduced compared to TC(4,8) (cf. **Fig. S 5**). With approximately 10%, the amount of unfolded species lies within the range of impurity determined by UHPLC-MS. The broad signals may therefore also correspond to unfolded Trp-containing side-products from the synthesis and not necessarily belong to unfolded switch-cage species.

3.2.2. Chemical shift deviations

The chemical shift deviation (CSD, also referred to as $\Delta\delta$) is typically employed to assess the stability of the fold of a Trp-cage mutant.[2,3] The CSD is the difference between the observed chemical shift of a certain nucleus in a peptide and the corresponding nucleus in an unstructured random coil peptide:

$$\text{CSD} = \Delta\delta = \delta_{\text{obs.}} - \delta_{\text{random coil}}$$

Unfortunately, we were unable to find a comprehensive list of random coil shifts used by Andersen *et al.*[2,3]. Therefore, random coil shifts were taken from Wishart *et al.* and are listed in **Tab. S 3**.[4] The random coil value of the Trp indole proton was taken from Bundi and Wüthrich.[5] The random coil shifts by Wishart *et al.* are non-stereospecifically assigned. When two β-protons ($H^{\beta 2/\beta 3}$) from the same residue display different random coil shifts, their CSD was calculated by subtracting the larger random coil shift from the larger observed shift and the smaller random coil shift from the smaller observed shift.

Example from Asp1:	Observed shift:	$H^{\beta 2/\beta 3}$: 2.881/2.714 ppm
	Random coil shift:	$H^{\beta 2/\beta 3}$: 2.72/2.65 ppm
	CSD:	$H^{\beta 2/\beta 3}$: 0.16/0.06 ppm

No CSDs are given for the acetyl moiety of the N-terminus and for residues Dpr4 and Dpr8 as no random coil values are available for their nuclei.

Tab. S 3: Random coil shifts used for the calculation of CSDs.

No.	Res.	Proton: CSD / ppm
00	Ac	Me: n.d.
01	D	H^{N}: 8.34, H^{α}: 4.64, $H^{\beta2/\beta3}$: 2.72/2.65
02	A	H^{N}: 8.24, H^{α}: 4.32, H^{β}: 1.39
03	Y	H^{N}: 8.12, H^{α}: 4.55, $H^{\beta2/\beta3}$: 3.03/2.98, H^{δ}: 7.14, H^{ε}: 6.84
04	Γ	n.d.
05	Q	H^{N}: 8.32, H^{α}: 4.34, $H^{\beta2/\beta3}$: 2.12/1.99, H^{γ}: 2.360, $H^{\varepsilon21/\varepsilon22}$: 7.52/6.85
06	W	H^{N}: 8.25, H^{α}: 4.66, $H^{\beta2/\beta3}$: 3.29/3.27, $H^{\delta1}$: 7.27, $H^{\varepsilon1}$: 10.22, $H^{\zeta2}$: 7.50, $H^{\eta2}$: 7.25, $H^{\varepsilon3}$: 7.65, $H^{\zeta3}$: 7.18
07	L	H^{N}: 8.16, H^{α}: 4.34, H^{β}: 1.62, H^{γ}: 1.59, $H^{\delta1/\delta2}$: 0.92/0.87
08	Γ	n.d.
09	D	H^{N}: 8.34, H^{α}: 4.64, $H^{\beta2/\beta3}$: 2.72/2.65
10	G	H^{N}: 8.33, H^{α}: 3.96
11	G	H^{N}: 8.21, H^{α}: 4.13
12	P	H^{α}: 4.42, $H^{\beta2/\beta3}$: 2.29/1.94, H^{γ}: 2.02, H^{δ}: 3.63
13	S	H^{N}: 8.31, H^{α}: 4.47, $H^{\beta2/\beta3}$: 3.89/3.87
14	S	H^{N}: 8.31, H^{α}: 4.47, $H^{\beta2/\beta3}$: 3.89/3.87
15	G	H^{N}: 8.33, H^{α}: 3.96
16	R	H^{N}: 8.20, H^{α}: 4.65, H^{β}: 1.81, H^{γ}: 1.67, H^{δ}: 3.21, H^{ε}: 8.07
17	P	H^{α}: 4.73, $H^{\beta2/\beta3}$: 2.31/1.91, H^{γ}: 2.01, H^{δ}: 3.60
18	P	H^{α}: 4.73, $H^{\beta2/\beta3}$: 2.31/1.91, H^{γ}: 2.01, H^{δ}: 3.60
19	P	H^{α}: 4.42, $H^{\beta2/\beta3}$: 2.29/1.94, H^{γ}: 2.02, H^{δ}: 3.63
20	S	H^{N}: 8.31, H^{α}: 4.47, $H^{\beta2/\beta3}$: 3.89/3.87

Tab. S 4: Chemical shift deviations of *cis*-SC_a.

No.	Res.	Proton: CSD / ppm
00	Ac	n.d.
01	D	H^{N}: -0.10, H^{α}: -0.02, $H^{\beta2/\beta3}$: 0.16/0.06
02	A	H^{N}: 0.45, H^{α}: -0.12, H^{β}: 0.09
03	Y	H^{N}: 0.59, H^{α}: -0.39, $H^{\beta2/\beta3}$: 0.17/0.15, H^{δ}: -0.02, H^{ε}: -0.05
04	Γ	n.d.
05	Q	H^{N}: 0.03, H^{α}: -0.42, $H^{\beta2/\beta3}$: 0.05/0.18, H^{γ}: 0.00, $H^{\varepsilon21/\varepsilon22}$: 0.17/0.02
06	W	H^{N}: -0.25, H^{α}: -0.42, $H^{\beta2/\beta3}$: 0.21/-0.08, $H^{\delta1}$: -0.26, **$H^{\varepsilon1}$: -0.49**, $H^{\zeta2}$: -0.27, $H^{\eta2}$: -0.10, $H^{\varepsilon3}$: -0.59, $H^{\zeta3}$: -0.03
07	L	H^{N}: 0.33, **H^{α}: -0.93**, $H^{\beta2/\beta3}$: 0.10/-0.28, H^{γ}: -0.07, $H^{\delta1/\delta2}$: -0.07/-0.22
08	Γ	n.d.
09	D	H^{N}: -0.47, H^{α}: -0.02, $H^{\beta2/\beta3}$: 0.17/0.03
10	G	H^{N}: -0.85, $H^{\alpha2/\alpha3}$: 0.19/-0.46
11	G	H^{N}: 0.08, **$H^{\alpha2/\alpha3}$: -1.01/-3.16**
12	P	H^{α}: 0.17, $H^{\beta2/\beta3}$: 0.23/0.13, H^{γ}: 0.12, $H^{\delta2/\delta3}$: 0.17/-0.21
13	S	H^{N}: -0.61, H^{α}: 0.00, $H^{\beta2/\beta3}$: 0.03/0.05
14	S	H^{N}: -0.13, H^{α}: -0.30, $H^{\beta2/\beta3}$: -0.02/-0.34
15	G	H^{N}: -0.40, $H^{\alpha2/\alpha3}$: 0.31/-0.15
16	R	H^{N}: -0.06, H^{α}: 0.37, $H^{\beta2/\beta3}$: 0.08/0.01, H^{γ}: -0.01, H^{δ}: 0.06, H^{ε}: -0.51
17	P	H^{α}: 0.02, $H^{\beta2/\beta3}$: 0.03/-0.11, H^{γ}: -0.01, $H^{\delta2/\delta3}$: 0.27/0.07
18	P	**H^{α}: -2.15**, **$H^{\beta2/\beta3}$: -0.96/-1.52**, $H^{\gamma2/\gamma3}$: -0.27/-0.36, H^{δ}: -0.08
19	P	H^{α}: -0.09, $H^{\beta2/\beta3}$: -0.09/0.04, H^{γ}: -0.16, $H^{\delta2/\delta3}$: -0.47/-0.64
20	S	H^{N}: -0.49, H^{α}: -0.31, $H^{\beta2/\beta3}$: -0.12/-0.10

Large CSDs which are a result of and an indicator for the stable Trp-cage fold are highlighted in bold.

3.3. Determination of midpoint of thermal unfolding of the switch cage

Fig 4a (in the paper) displays data of thermal unfolding of the switch cage (black circles). The following function was fitted to the data

$$y = A_2 + \frac{A_1 - A_2}{1 + exp(\frac{x - x_0}{dx})}$$

yielding the following values: A_1 = -13518.25883 ± 404.28719
A_2 = -3855.61105 ± 228.37507
x_0 = 48.50329 ± 1.42176 (in this case $x_0 = T_m$)
dx = 12.95674 ± 1.42566

4. Switching properties of the switch cage

4.1. UV/vis spectroscopy

UV/vis spectra were recorded at 25 °C on a Lambda 14 spectrometer (PerkinElmer, Waltham, MA, USA) equipped with a ecoline E100 thermostat mounted on an ecoline 003 water bath (Lauda, Lauda-Königshofen, Germany). Measurements were performed using low-volume (700 µL) Quartz cuvettes with an optical path length of 10 mm (Hellma, Müllheim, Germany) and water as a solvent at pH = 5.5 ± 0.1.

UV/vis spectroscopy was used to determine the which of the available light sources produces the largest *cis*→*trans*-conversion ratio (**Fig. S 12**). From the tested wavelengths, the highest conversion to *trans*-SC was achieved at 385 nm.

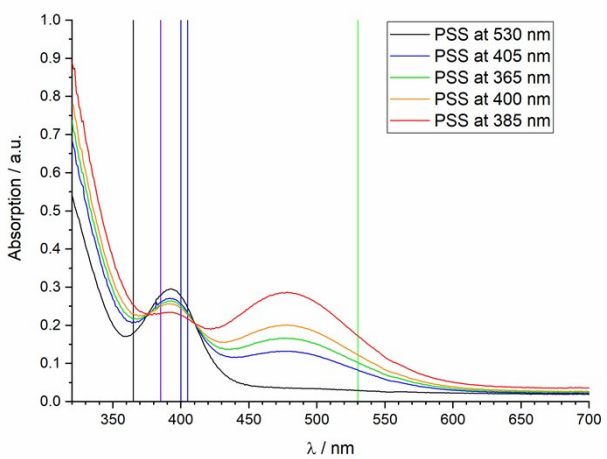

Fig. S 12: UV/vis spectra of the switch cage irradiated with light of different wavelengths (365 nm, 385 nm, 400 nm, 405 nm and 530 nm). The irradiation wavelengths are indicated by a vertical line. The baseline displays a small offset which is an artifact resulting from the narrow low-volume cuvettes.

4.2. Photostationary state at 385 nm and relaxation rates

4.2.1. Experimental setup

The photostationary state (PSS) and relaxation rate were determined by NMR spectroscopy. The sample with the switch cage was irradiated to the PSS at 385 nm and immediately afterwards a 1D-^{1}H-NMR spectrum was recorded (**Fig. S 13**). The NMR spectrometer had previously been calibrated to a temperature of 298 °C. The sample remained in the spectrometer in the dark for the entire time of the relaxation measurements. After the first spectrum (representing the PSS, recorded at t = 2 min after irradiation), a new spectrum was recorded every 30 min for the next 21 h. The last spectrum was recorded at t = 39 h.

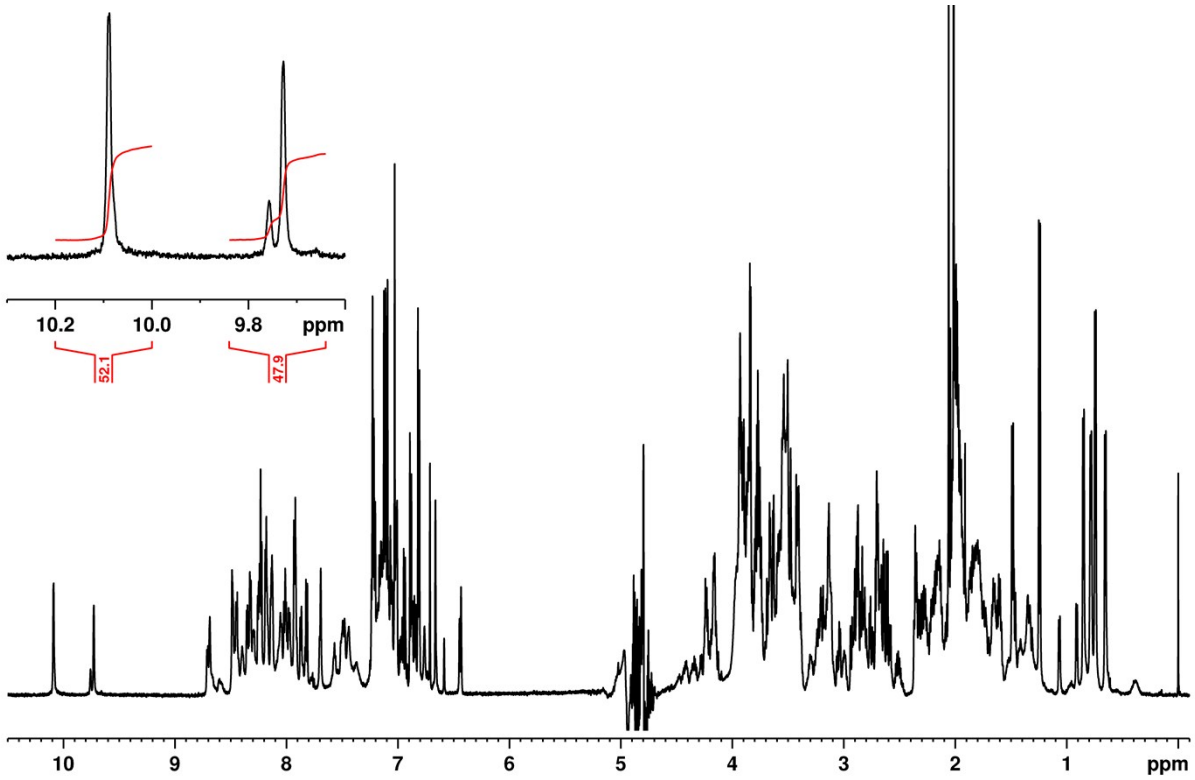

Fig. S 13: 1D-^{1}H-NMR spectrum of the switch cage after irradiation to the PSS at 385 nm in water with 10% D_2O at pH = 5.5, 298 K and a concentration of 0.5 mM. The same regions as in **Fig. S 11** are integrated in the expansion.

4.2.2. Selecting the nuclei for the determination of the PSS at 385 nm and the relaxation rate

Accurate determination of photostationary states and relaxation rates ideally requires baseline-separated signals of the *cis*- and the *trans* diazocine to allow for integration. Unfortunately, all signals of the *trans*-diazocine overlap with other aromatic signals of *trans*-SC, *cis*-SC_a or *cis*-SC_b. In consequence, six largely separated signals of *cis*-SC (signals b) – g)) and one signal (signal a)) of *trans*-SC were used to quantify the *cis*- and *trans*-populations and determine the relaxation rate (**Tab. S 5**, **Fig. S 14**).

The six chosen *cis*-SC-signals (b) – g)) represent either the switching state of the diazocine cross-linker or the fold state of the switch cage (**Tab. S 5**). This facilitates the discrimination between the state of the linker and the fold and it also allows for the determination of the PSS and relaxation rates for each

individual species, i.e. *cis*-SC_a and *cis*-SC_b. Signal a) was chosen to calculate the relaxation rate by monitoring a fold-indicating proton of *trans*-SC.

Tab. S 5: List of signals that were chosen to calculate the PSS and/or the relaxation rate of the switch cage.

Entry	Species	Proton	Integr. Region / ppm	Representing
a)	*trans*-SC	Trp6 indole NH	10.105 – 10.065	fold
b)	*cis*-SC_b	Trp6 indole NH	9.780 – 9.744	fold
c)	*cis*-SC_a	Trp6 indole NH	9.744 – 9.700	fold
d)	*cis*-SC_a	Dpr4 H^2	6.725 – 6.699	diazocine
e)	*cis*-SC_a	Dpr8 H^2	6.692 – 6.632	diazocine
f)	*cis*-SC_b	DprX H^2*	6.600 – 6.570	diazocine
g)	*cis*-SC_a: Dpr8 H^4; *cis*-SC_b: Dpr H^2**		6.473 – 6.413	diazocine

*) It was not possible to unequivocally assign the two protons, Dpr4 H^2 and Dpr8 H^2 of *cis*-SC_b, to their corresponding residue in the sequence. **) These two signals are overlapping and treated as one.

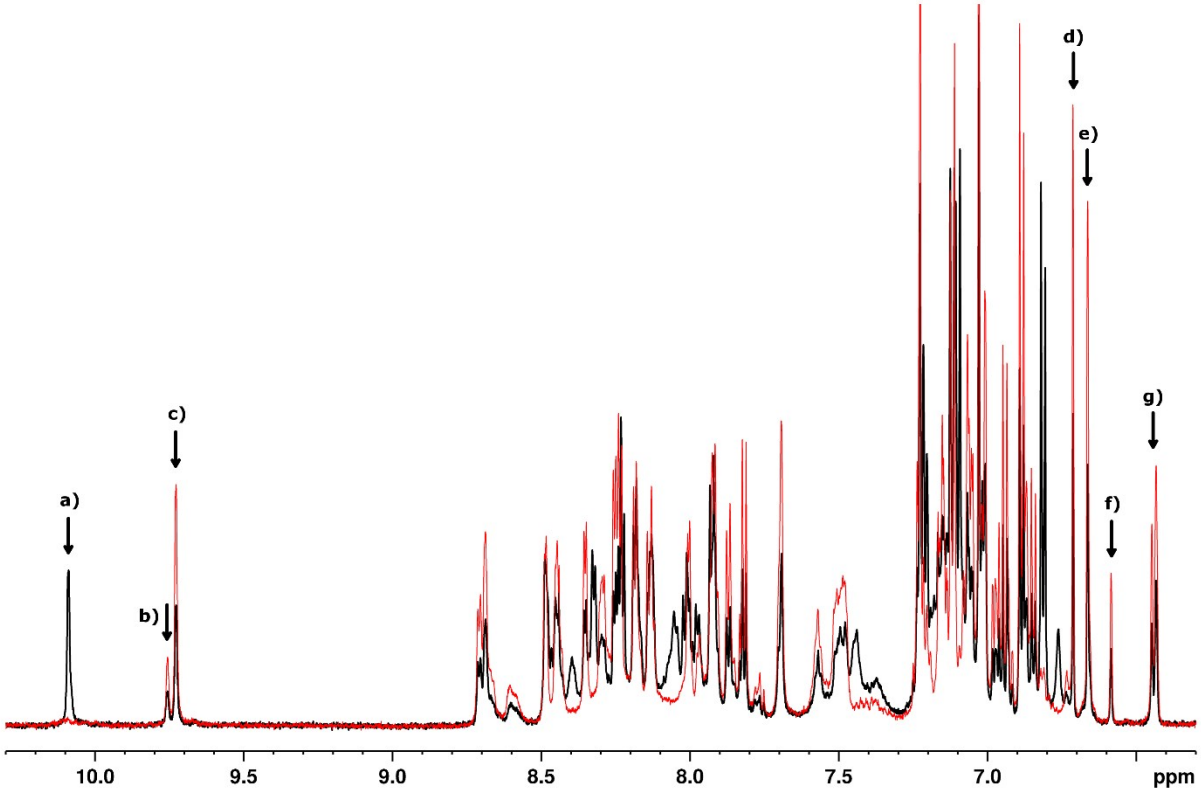

Fig. S 14: The indole, amide and aromatic region of the 1D-^{1}H-NMR spectra of the switch cage after irradiation to the PSS at 385 nm (red) and relaxation in the dark at 298 K for 39 h (black) are shown. The full spectra are depicted in **Fig. S 13** (PSS at 385 nm) and **Fig. S 11** (dark-adapted). The signals marked a) – g) were chosen for determination of the PSS and relaxation rates as they are more or less baseline-separated.

4.2.3. Determination of the PSS at 385 nm

The PSS at 385 nm was determined *via* the six signals of *cis*-SC (Signals b) – g) of **Tab. S 5** and **Fig. S 14**). The ratio of their intensity after irradiation to the PSS at 385 nm ($I_{385\ nm}$) and their intensity in the dark-adapted state ($I_{dark\text{-}adapted}$) is correlated to the *cis*→*trans*-conversion ratio in the PSS according to the following formula:

$$1 - \frac{I_{385\,nm}}{I_{dark-adapted}} = \textit{cis}\rightarrow\textit{trans}\text{-conversion ratio}$$

Note that this method can only be applied with signals of *cis*-SC, as signals of *trans*-SC are essentially zero in the dark-adapted state.

The first (recorded at t = 2 min after irradiation) and the last spectrum (t = 39 h) of the relaxation measurements were chosen to represent the PSS and the dark-adapted state, respectively. In order to determine the PSS, the intensity of signals b) – g) (**Tab. S 5**, **Fig. S 14**) was measured by integration. Their integrals were calibrated relative to the DSS integral which was arbitrarily set to 1. The obtained intensities were inserted in the formula to obtain the approximate fraction of *trans*-SC in the PSS listed in **Tab. S 6**.

4.2.4. Determination of the relaxation rate

In order to determine the relaxation rate, every 1D-^{1}H-NMR spectrum of the relaxation measurements was integrated within the ranges listed in **Tab. S 5** (signals a) – g)). These integrals were calibrated relative to the DSS signal, which was arbitrarily set to 1. The signal intensity was plotted over the time (**Fig. S 15**) and the following function of exponential decay was fitted to the data:

$$y = A_1 \cdot e^{\left(\frac{-x}{t_1}\right)} + y_0$$

In this formula, x is the time, y_0 is the offset to which the function approaches asymptotically, t_1 is the time constant of the decay and A_1 is the initial decaying quantity. The sum of y_0 and A_1 ($y_0 + A_1$) give the y-intercept (initial total quantity). The half-life $t_{1/2}$ was calculated by the following relationship:

$$t_{1/2} = t_1 \cdot ln(2)$$

The results of the fitted data are listed in the table included in **Fig. S 15**, the final results are listed in **Tab. S 6**.

4.2.5. Results

Tab. S 6: Resulting PSS and relaxation rate from each signal a) – g).

Entry	Species	Representing	$PSS_{385\,nm}$ / % *trans*-state	$t_{1/2}$ / h
a)	*trans*-SC	fold	n.d.	6.7 ± 0.1
b)	*cis*-SC_b	fold	43	5.6 ± 0.3
c)	*cis*-SC_a	fold	49	6.1 ± 0.1
d)	*cis*-SC_a	diazocine	46	6.5 ± 0.1
e)	*cis*-SC_a	diazocine	45	6.3 ± 0.2
f)	*cis*-SC_b	diazocine	46	6.5 ± 0.3
g)	*cis*-SC_a / *cis*-SC_b	diazocine	47	6.0 ± 0.2
		Average:	**46 ± 2**	**6.2 ± 0.3**

There is no significant discrepancy in the PSS or half-life of either species, i.e. *cis*-SC_a, *cis*-SC_b or *trans*-SC, nor is there any significant deviation between the behavior of the fold and the diazocine. This implies a direct coupling of the fold and the photoswitchable cross-linker.

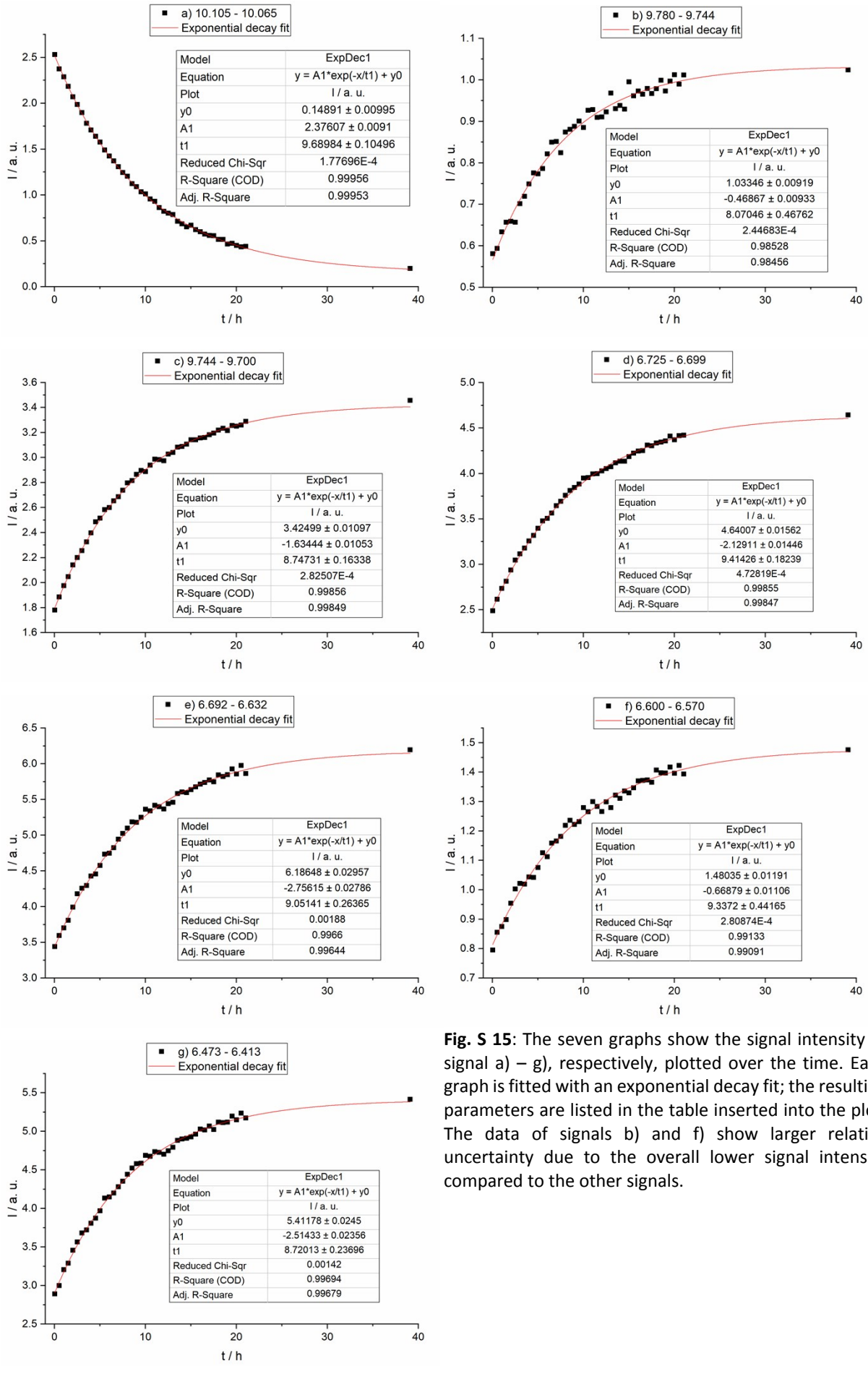

Fig. S 15: The seven graphs show the signal intensity of signal a) – g), respectively, plotted over the time. Each graph is fitted with an exponential decay fit; the resulting parameters are listed in the table inserted into the plot. The data of signals b) and f) show larger relative uncertainty due to the overall lower signal intensity compared to the other signals.

4.3. Photostationary state at 530 nm

The 1D-^{1}H-NMR spectrum of the switch-cage recorded immediately after irradiation to the PSS at 530 nm is virtually identical the spectra of the dark-adapted switch-cage (**Fig. S 16**). Therefore, irradiation with light of the wavelength 530 nm affords nearly complete conversion to the *cis*-switch cage.

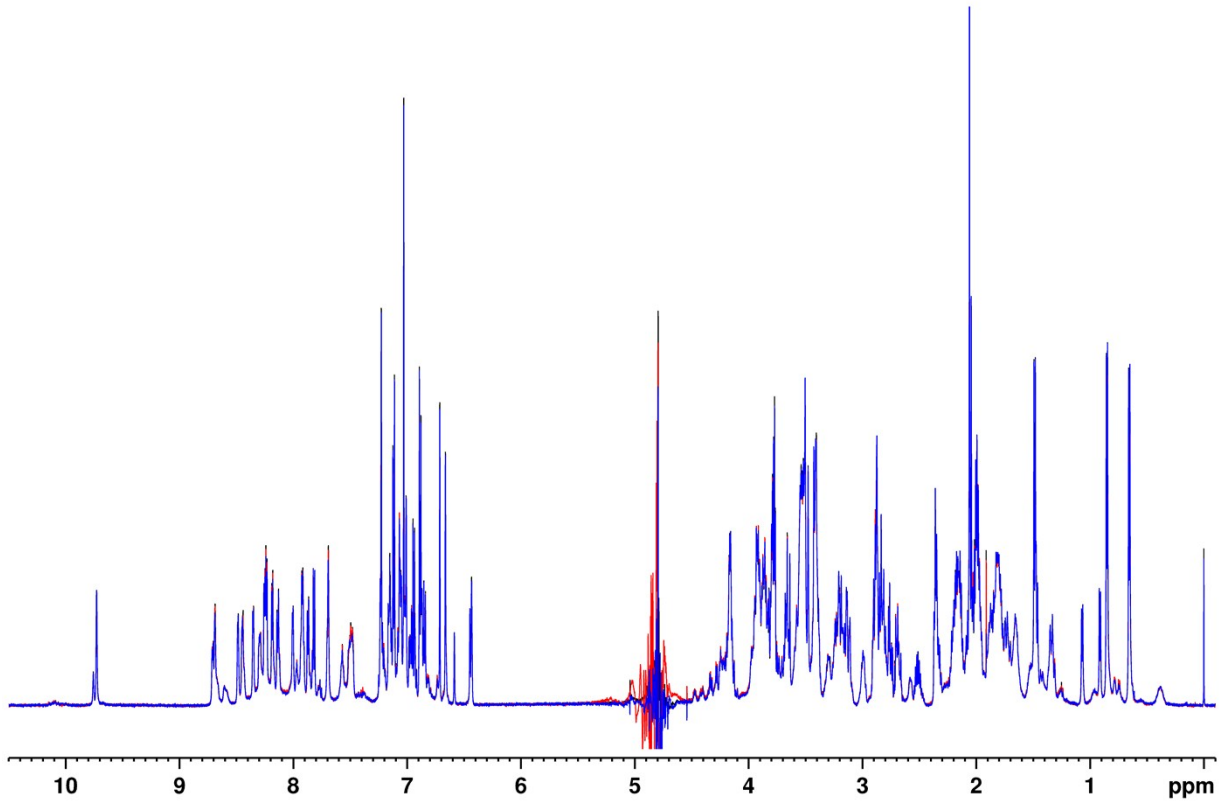

Fig. S 16: Overlay of the 1D-^{1}H-NMR spectra of dark-adapted *cis*-SC as obtained after purification (black), *cis*-SC immediately after irradiation to the PSS at 530 nm (red), and *cis*-SC after irradiation to the PSS at 385 nm and subsequent relaxation in the dark at 298 K (24.85 °C) for 39 h (blue). Apart from the water suppression artifact around 4.9 ppm, the three spectra are virtually identical.

4.4. Mechanism of interconversion between *cis*-SC_a and *cis*-SC_b

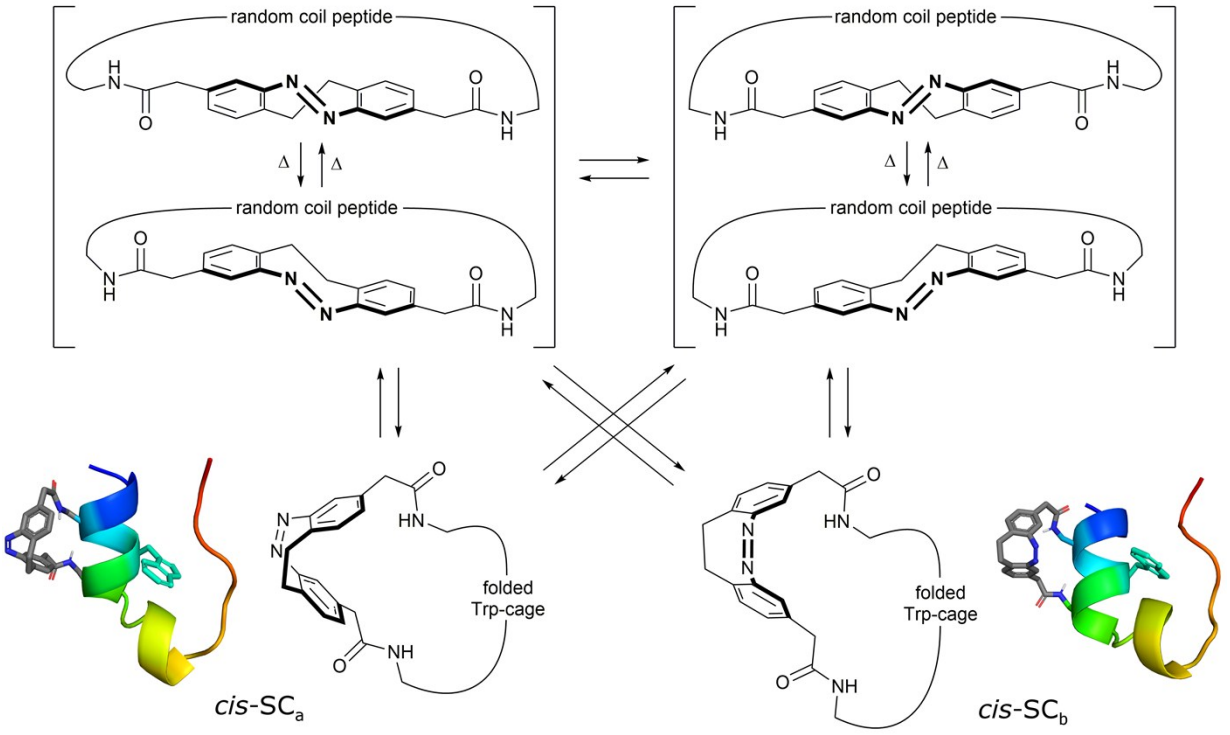

Scheme S 1: Mechanism of interconversion between *cis*-SC_a, *cis*-SC_b and the two diastereomers of *trans*-SC in the twist and chair conformation. Deltas (Δ) indicate thermal interconversion at ambient temperature. The other indicated equilibria are significantly slower and require higher temperatures or irradiation with light.

5. Cross-linker synthesis and characterization

5.1. Devices

5.1.1. Chromatography stationary phases

Flash column chromatography purfications were performed on a Biotage Isolera one with Biotage Ultra cartridges (HP-Sphere, particle diameter: 25 µm, cartridge sizes: 10 g, 25 g, 50 g and 100 g; Biotage, Uppsala, Sweden). R_f values were determined by thin layer chromatography on Polygram SilG/UV_{254} (0.2 mm particle size; Macherey-Nagel, Düren, Germany) and ALUGRAM Xtra SIL G/UV_{254} (0.2 mm particle size; Macherey-Nagel, Düren, Germany).

5.1.2. Melting point determination

Melting points were measured with a B-560 Melting Point Apparatus (Büchi, Essen, Germany) in melting point tubes.

5.1.3. NMR spectroscopy

NMR measurements of the cross-linker and its precursors were performed with a Bruker DRX 500 FT-NMR spectrometer (^{1}H-NMR: 500.1 MHz, ^{13}C-NMR: 125.8 MHz; Bruker, Billerica, MA, USA).

NMR spectra were measured in deuterated solvents (Deutero, Kastellaun, Germany). Spectra were referenced to TMS when acetone, acetonitrile or chloroform was the solvent. Otherwise the following solvent signals were used for referencing:

Tab. S 7: List of deuterated solvents.

Solvent	**Degree of deuteration**	**^{1}H signal**	**^{13}C signal**
Acetone-d_6	99.8%	2.05 (quintet)	29.84 (septet)
Acetonitrile-d_3	99.8%	1.94 (quintet)	118.26 (septet)
Chloroform-d_1	99.8%	7.26 (s)	77.16 (triplet)
DMSO-d_6	99.8%	2.50 (s)	39.52 (septet)
Methanol-d_4	99.8%	3.34 (s)	49.86 (septet)

5.1.4. IR spectroscopy

Infrared spectra were measured on a PerkinElmer 1600 Series FT-IR spectrometer with an A531-G Golden-Gate-Diamond-ATR-unit (PerkinElmer, Waltham, MA, USA). Signals were abbreviated with w for weak, m for medium and s for strong signal intensity.

5.1.5. Mass spectrometry

The high resolution-electron ionization (HR-EI) mass spectra were measured with an AccuTOF GCv 4G (Jeol Germany, Freising, Germany) with ionization energy of 70 eV and the high resolution-electrospray ionization (HR-ESI) mass spectra were measured with a Q Exactive Plus MS, Hybrid Quadrupol-Orbitrap (Thermo Fisher Scientific, Waltham, MA, USA).

5.2. Synthetic procedures and analysis results

General remark:

The 4-methyl-2,6,7-trioxabicyclo[2.2.2]octane-1-yl (OBO) protecting group that was employed during the cross-linker synthesis is highly labile against acids and a fraction may unintentionally be hydrolyzed to the open ester during the work-up of reaction ii) or iii) of **Scheme 2** in the paper.

5.2.1. Synthesis of (3-methyloxetan-3-yl)methyl 2-(4-methyl-3-nitrophenyl)acetate (8)

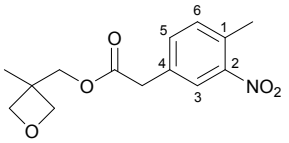

At 0 °C and under N_2 atmosphere 2-(4-methyl-3-nitrophenyl)acetic acid (**6**; 3.9 g, 20 mmol), 4-dimethylaminopyridine (DMAP; 244 mg, 2 mmol) and *N*,*N*'-dicyclohexylcarbodiimide (DCC; 4.13 g, 20 mmol) were dissolved in 30 ml dry dichloromethane (DCM). Immediately afterwards 3-methyl-3-oxetanemethanol (**7**; 1.98 ml, 20 mmol) was added. The reaction was stirred for 1 h at room temperature. The formed solid was filtered and washed with 100 ml DCM. The solvent was evaporated in vacuo and the crude product was purified by flash column chromatography (cyclohexane/ethyl acetate) to afford the product as a yellow oil (4.91 g, 17.6 mmol, 88%).

R_f: 0.29 (cyclohexane/ethyl acetate, 2:1).

^{1}H-NMR (500.1 MHz, Acetone-d_6, 300 K): δ = 7.96 (d, ^4J = 1.8 Hz, 1 H, *H*-3), 7.58 (dd, ^3J = 8.0 Hz, ^4J = 1.7 Hz, 1 H, *H*-5), 7.44 (d, ^3J = 7.8 Hz, 1 H, *H*-6), 4.41 (d, ^4J = 5.8 Hz, 2 H, C-CH_2-O-), 4.25 (d, ^4J = 5.8 Hz, 2 H, C-CH'_2-O-), 4.21 (s, 2 H, C-CH_2-OOC), 3.87 (s, 2 H, OOC-CH_2-C_4), 2.54 (s, 3H, C_1-CH_3), 1.29 (s, 3H, C-CH_3) ppm.

^{13}C-NMR (125.8 MHz, Acetone-d_6, 300 K): δ = 171.4 (*C*OO), 150.1 (*C*-2), 135.2 (*C*-5), 135.1 (C-4), 133.6 (*C*-6), 132.4 (C-1), 126.1 (*C*-3), 79.6 (*C*-CH_2-O-), 70.0 (C-*C*H_2-OOC), 40.2 (OOC-*C*H_2-C_4), 21.2 (C-*C*H_3), 19.7 (C_1-*C*H_3) ppm.

IR (ATR): $\tilde{\nu}$ = 2963 (w), 2872 (w), 1735 (s), 1526 (s), 1498 (w), 1454 (w), 1346 (s), 1298 (w), 1246 (m), 1223 (m), 1152 (s), 1031 (w), 977 (s), 833 (m), 815 (s), 751 (w), 732 (w), 678 (w) cm^{-1}.

MS (EI, 70 eV): m/z (%) = 279 (7), 262 (5), 196 (5), 177 (13), 150 (100).

HRMS (EI, 70 eV): $[C_{14}H_{17}N_1O_5]^+$, calc.: m/z = 279.11067, found: m/z = 279.11046.

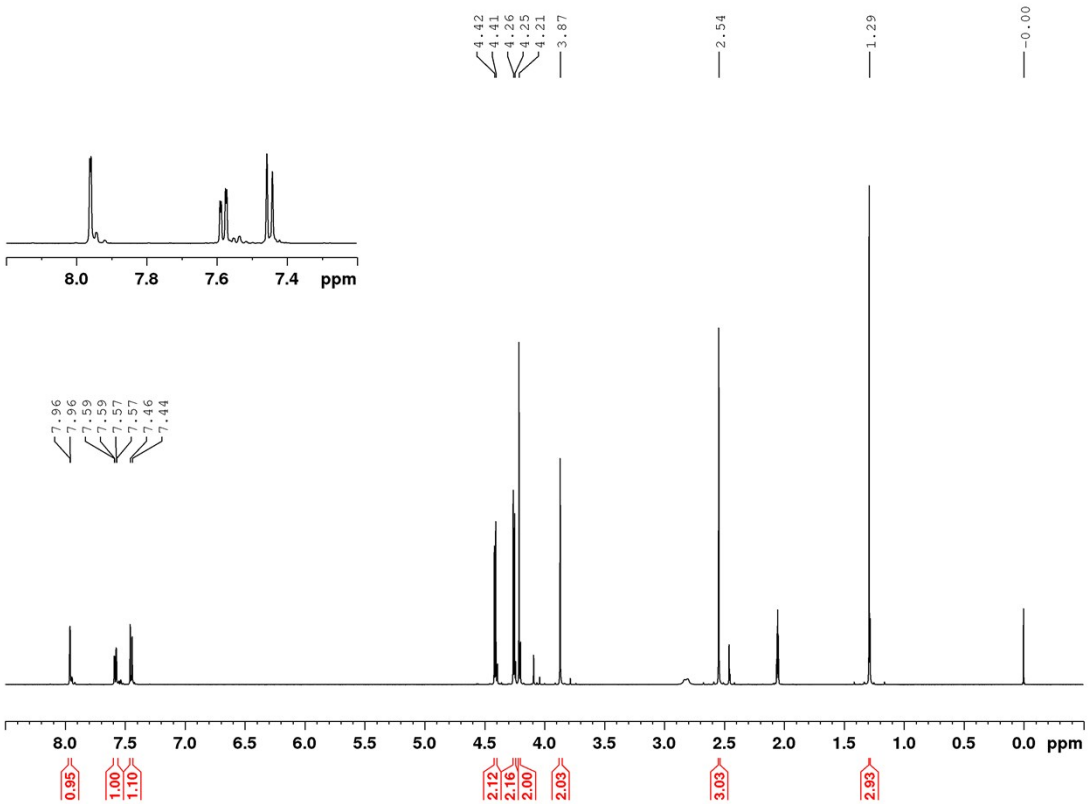

Fig. S 17: ^{1}H-NMR spectrum of compound **8** measured in deuterated acetone at 300 K.

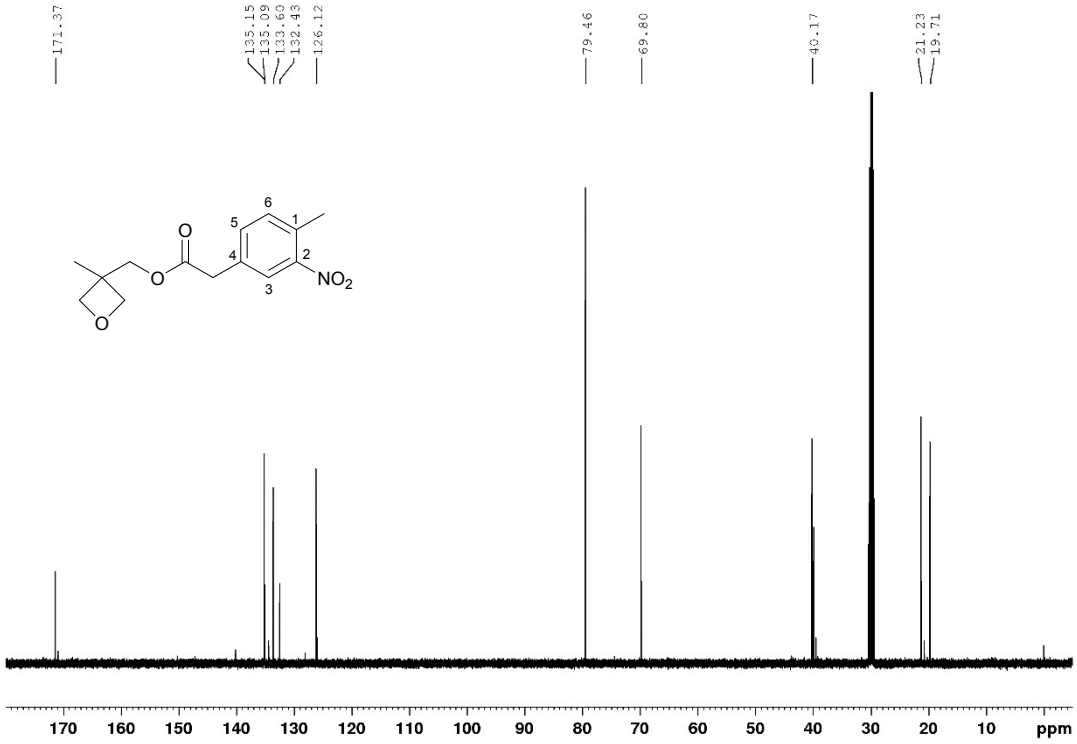

Fig. S 18: ^{13}C-NMR spectrum of compound **8** measured in deuterated acetone at 300 K.

5.2.2. Synthesis of 4-methyl-1-(4-methyl-3-nitrobenzyl)-2,6,7-trioxabicyclo[2.2.2]octane (9)

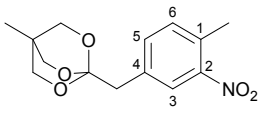

Under N_2 atmosphere (3-methyloxetan-3-yl)methyl 2-(4-methyl-3-nitrophenyl)acetate (**8**; 2.00 g, 7.16 mmol) was dissolved in 20 ml dry DCM, cooled to -10 °C and 48% $BF_3{\cdot}Et_2O$ solution (200µl, 716 µmol) was added dropwise. The reaction was stirred at room temperature for 2 h and stopped with trimethylamine (TEA; 1.00 ml, 7.16 mmol). The solvent was evaporated in vacuo and the residue was dissolved in ethyl acetate. The organic layer was washed with 5% ammonium chloride solution (150 ml), H_2O (2 x 100 ml), saturated sodium bicarbonate solution (2 x 100 ml), saturated sodium chloride solution (100 ml) and dried over magnesium sulfate. The solvent was evaporated in vacuo and the crude product was purified by flash column chromatography (cyclohexane/ethyl acetate, 1:2) to afford the product as colourless crystals (1.61 g, 5.79 mmol, 81%).

R_f: 0.48 (cyclohexane/ethyl acetate, 2:1).

T_m: 118 °C

^{1}H-NMR (500.1 MHz, Acetone-d_6, 300 K): δ = 7.85 (d, ^4J = 1.7 Hz, 1 H, *H*-3), 7.47 (dd, ^3J = 7.9 Hz, ^4J = 1.78 Hz, 1 H, *H*-5), 7.34 (d, ^3J = 7.9 Hz, 1 H, *H*-6), 3.86 (s, 6 H, C-CH_2-O-), 2.98 (s, 2 H, C-CH_2-C_4), 2.52 (s, 3H, C_1-CH_3), 0.79 (s, 3H, C-CH_3) ppm.

^{13}C-NMR (125.8 MHz, Acetone-d_6, 300 K): δ = 149.8 (*C*-2), 136.3 (*C*-5), 136.1 (C-4), 132.8 (*C*-6), 132.4 (C-1), 127.0 (*C*-3), 108.9 (O-*C*-CH_2), 73.1 (C-*C*H_2-O-), 42.5 (C-*C*H_2-C_4), 31.1 (*C*-CH_3), 19.7 (C_1-*C*H_3), 14.3 (C-*C*H_3).

IR (ATR): $\tilde{\nu}$ = 2966 (w), 2935 (w), 2886 (w), 1733 (m), 1526 (s), 1472 (w), 1464 (w), 1453 (w), 1440 (w), 1397 (w), 1384 (w), 1340 (w), 1309 (m), 1282 (m), 1264 (m), 1207 (m), 1190 (m), 1153 (m), 1043 (s), 1025 (s), 1011 (s), 984 (s), 928 (m), 923 (m), 895 (m), 886 (m), 851 (m), 837 (m), 818 (m), 768 (w), 755 (w), 718 (s), 688 (w), 675 (w) cm^{-1}.

MS (EI, 70 eV): m/z (%) = 279 (3), 249 (37), 179 (20), 150 (100).

HRMS (EI, 70 eV): $[C_{14}H_{17}N_1O_5]^+$, calc.: m/z = 279.11067, found: m/z = 279.11090.

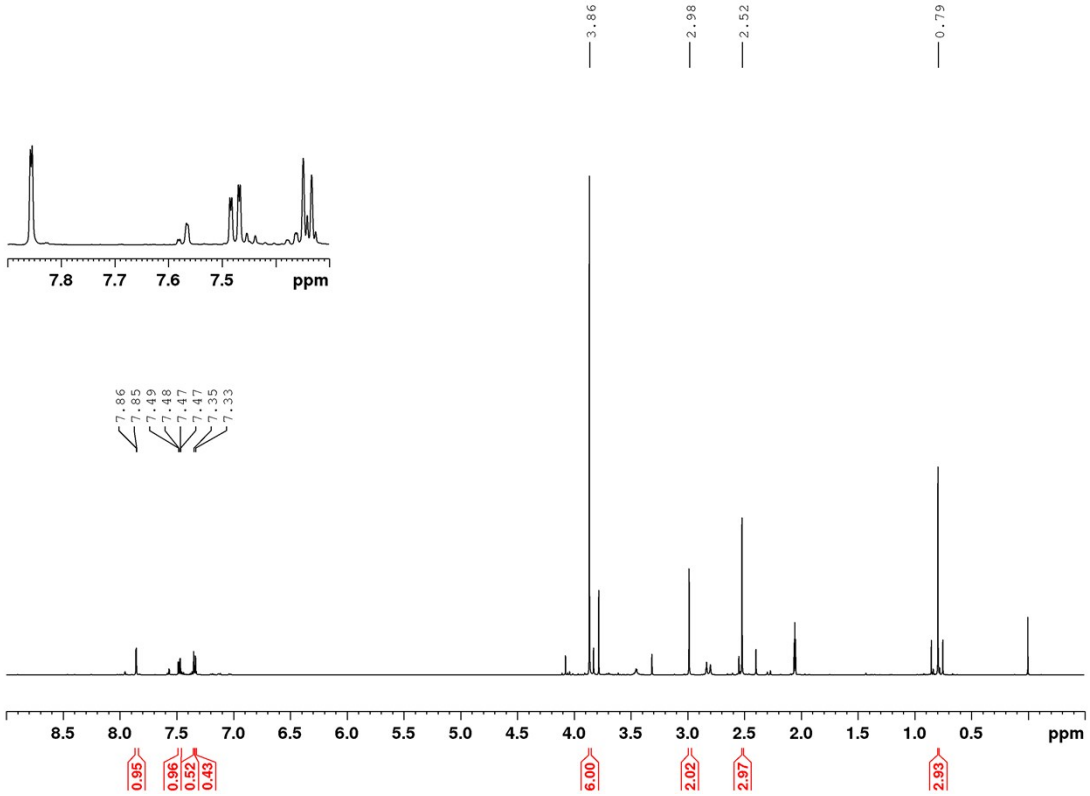

Fig. S 19: ^{1}H-NMR spectrum of compound **9** measured in deuterated acetone at 300 K.

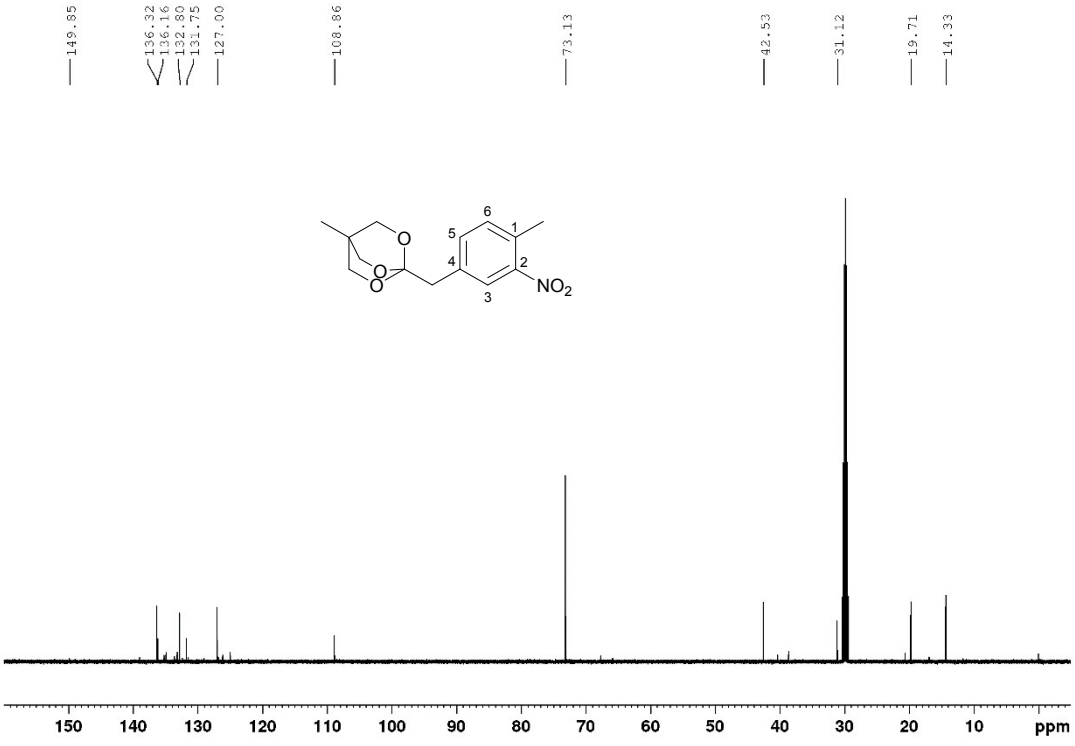

Fig. S 20: ^{13}C-NMR spectrum of compound **9** measured in deuterated acetone at 300 K.

5.2.3. Synthesis of 1,2-bis(4-((4-methyl-2,6,7-trioxabicyclo[2.2.2]octan-1-yl)methyl)-2-nitrophenyl)ethane (10)

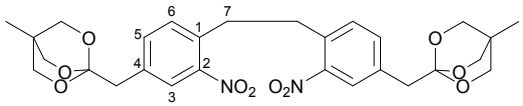

Under N_2 atmosphere 4-methyl-1-(4-methyl-3-nitrobenzyl)-2,6,7-trioxabicyclo[2.2.2]octane (**9**; 1.50 g, 5.37 mmol) was dissolved in 30 ml dry tetrahydrofuran (THF) and cooled to -5 °C, followed by addition of potassium butoxide (1.02 g, 9.13 mmol). The reaction was stirred for 40 s before addition of bromine (274 µl, 5.37 mmol). After further stirring for 10 min at room temperature the reaction mixture was added to a saturated sodium bicarbonate solution and extracted with ethyl acetate (3 x 100 ml). The combined organic layers were washed with 100 ml saturated sodium thiosulfate solution and dried over magnesium sulfate. The solvent was evaporated in vacuo and the crude product was purified by flash column chromatography (cyclohexane/ethyl acetate, 2:1) to afford the product as colourless crystals (680 mg, 2.44 mmol, 46%).

R_f: 0.28 (cyclohexane/ethyl acetate, 2:1).

T_m: 116 °C

^{1}H-NMR (500.1 MHz, Acetone-d_6, 300 K): δ = 7.86 (d, ^4J = 1.7 Hz, 2 H, *H*-3), 7.55 (dd, ^3J = 7.9 Hz, ^4J = 1.8 Hz, 2 H, *H*-5), 7.42 (d, ^3J = 7.9 Hz, 2 H, *H*-6), 3.87 (s, 12 H, C-CH_2-O-), 3.20 (s, 4 H, C-CH_2-C_4), 3.01 (s, 4H, *H*-7), 0.80 (s, 6H, C-CH_3) ppm.

^{13}C-NMR* (125.8 MHz, Acetone-d_6, 300 K): δ = 149.8 (*C*-2), 136.5 (*C*-5), 136.8 (*C*-4), 134.5 (*C*-1), 132.1 (*C*-6), 127.2 (*C*-3), 108.9 (O-*C*-CH_2), 73.1 (C-*C*H_2-O-), 42.6 (C-*C*H_2-C_4), 34.2 (*C*-7), 31.1 (*C*-CH_3), 14.3 (C-*C*H_3).

IR (ATR): $\tilde{\nu}$ = 3310 (w), 2883 (w), 1726 (s), 1526 (w), 1525 (s), 1458 (w), 1341 (s), 1227 (m), 1169 (s), 1038 (s), 1002 (s), 924 (s), 846 (s), 817 (m), 764 (w), 732 (w), 679 (m) cm^{-1}.

MS (EI, 70 eV): m/z (%) = 556(8), 539 (9), 294 (32), 278 (100).

HRMS (EI, 70 eV): $[C_{28}H_{32}N_2O_{10}]^+$, calc.: m/z = 556.20569, found: m/z = 556.20124.

*Frequencies were determined from the carbon dimension of the HMBC spectrum.

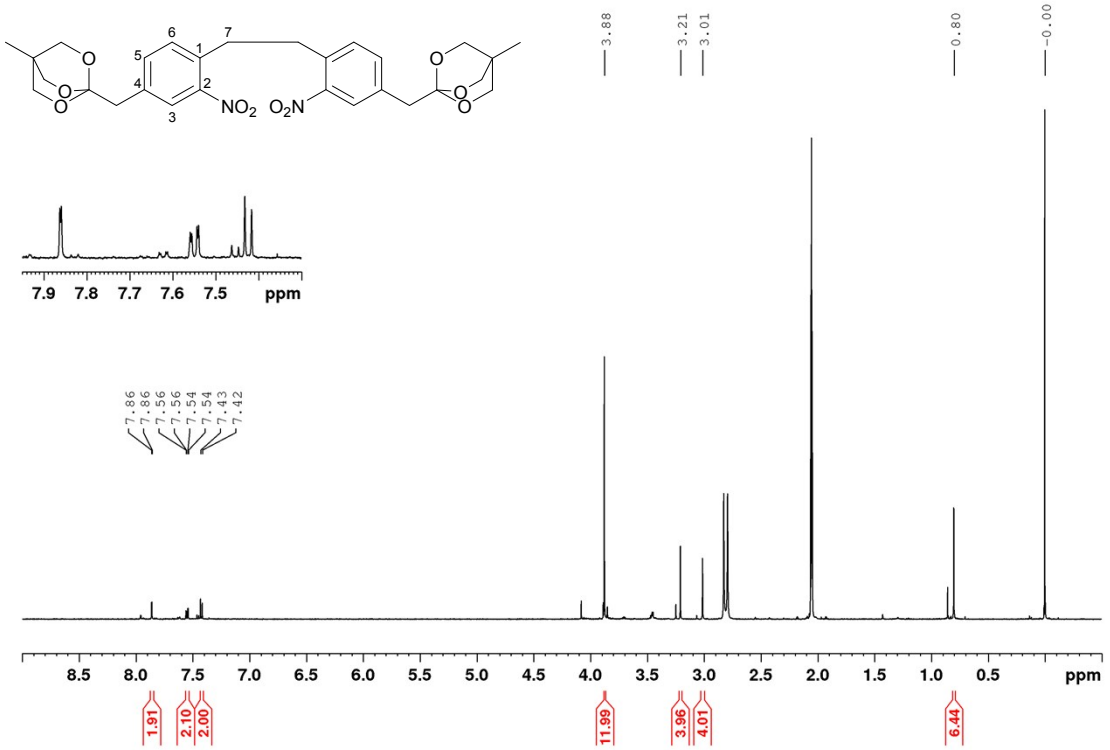

Fig. S 21: ^{1}H-NMR spectrum of compound **10** measured in deuterated acetone at 300 K.

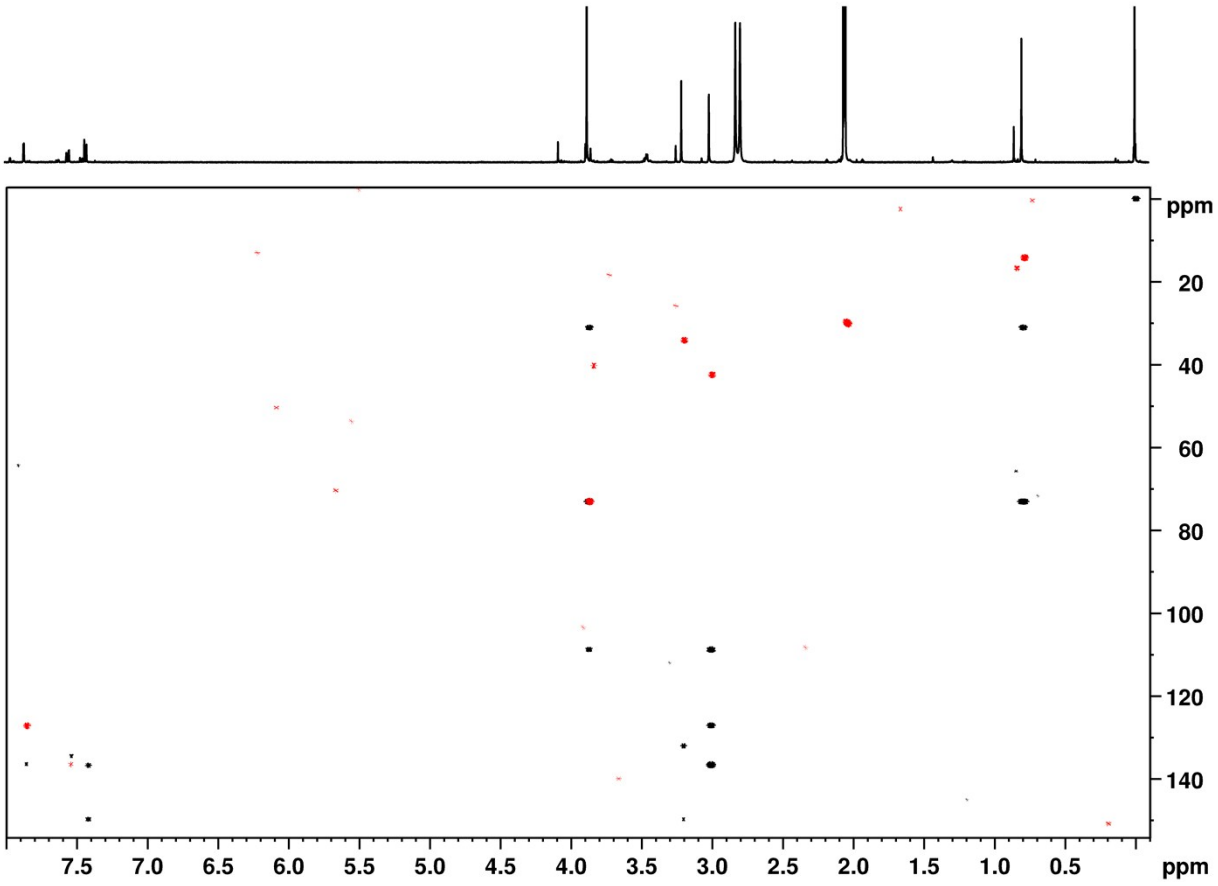

Fig. S 22: Overlay of the ^{1}H,^{13}C-HSQC (red) and the ^{1}H,^{13}C-HMBC (black) of compound **10** measured in deuterated acetone at 300 K.

5.2.4. Synthesis of (Z)-bis(3-hydroxy-2-(hydroxymethyl)-2-methylpropyl) 2,2'-(11,12-dihydro-dibenzo[c,g][1,2]diazocine-3,8-diyl)diacetate (11)

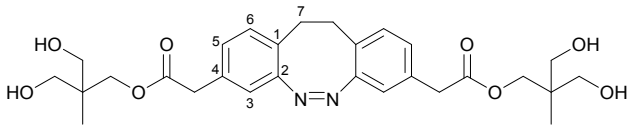

A mixture of 1,2-bis(4-((4-methyl-2,6,7-trioxabicyclo[2.2.2]octan-1-yl)methyl)-2-nitrophenyl)ethane (**10**; 431 mg, 775 µmol), $Ba(OH)_2 \cdot 8\ H_2O$ (732 mg, 2.33 mmol) and zinc powder (811 mg, 12.4 mmol) were dissolved in an ethanol-water mixture (60 ml, 2:1) and stirred for 5 h under reflux. After filtration trough Celite and evaporation of the solvent under reduced pressure, the crude product was dissolved in 90 ml 0.1 M methanolic NaOH solution, $CuCl_2$ (20 mg, 149 µmol) was added, and air was blown trough the solution for 4 h. The reaction was added to a saturated sodium bicarbonate solution, neutralized with 1 M HCl solution and extracted with DCM (3 x 75 ml). The combined organic layers were washed with a saturated sodium chloride solution and dried over magnesium sulfate. The solvent was evaporated in vacuo and the crude product was purified by flash column chromatography (cyclohexane/ethyl acetate, 2:1) to afford the product as a yellow solid (161 mg, 326 µmol, 42%).

R_f: 0.22 (cyclohexane/ethyl acetate, 2:1).

T_m: 132 °C

^{1}H-NMR (500.1 MHz, $CDCl_3$, 300 K): δ = 6.96 (s, 4 H, *H*-5, *H*-6), 6.79 (d, ^3J = 7.9 Hz, 2 H, *H*-3), 4.13 (s, 4 H, COO-CH_2-C), 3.57 (s, 4 H, COO-CH_2-C_4), 3.44 (d, ^3J = 11.4 Hz, 4 H, CH_2-OH), 3.36 (d, ^3J = 11.4 Hz, 4 H, CH'_2-OH), 2.85 (s, 4 H, *H*-7), 2.41 (s, 4H, CH_2-O*H*), 0.71 (s, 6H, C-CH_3) ppm.

^{13}C-NMR (125.8 MHz, $CDCl_3$, 300 K): δ = 172.0 (*C*OO), 155.3 (*C*-2), 132.5 (*C*-4), 130.0 (*C*-5), 128.1 (*C*-5), 127.0 (*C*-1), 125.6 (*C*-5), 119.8 (*C*-3), 67.5 (CH_3-*C*-$(CH_2)_3$) 67.4 (*C*H_2-OH) 66.9 (COO-*C*H_2-C), 40. (COO-*C*H_2-C_4), 31.4 (*C*-7), 16.7(C-*C*H_3) ppm.

IR (ATR): $\tilde{\nu}$ = 3312 (w), 2933 (w), 2880 (w), 1730 (s), 1458 (w), 1396 (w), 1334 (m), 1303 (m), 1253 (m), 1191 (m), 1151 (w), 1038 (s), 990 (s), 892 (w), 835 (w), 702 (w) cm^{-1}.

HRMS (HR-ESI): $[C_{28}H_{36}O_8N_2 + NH_4]^+$, calc.: m/z = 546.2806, found: m/z = 546.28099.

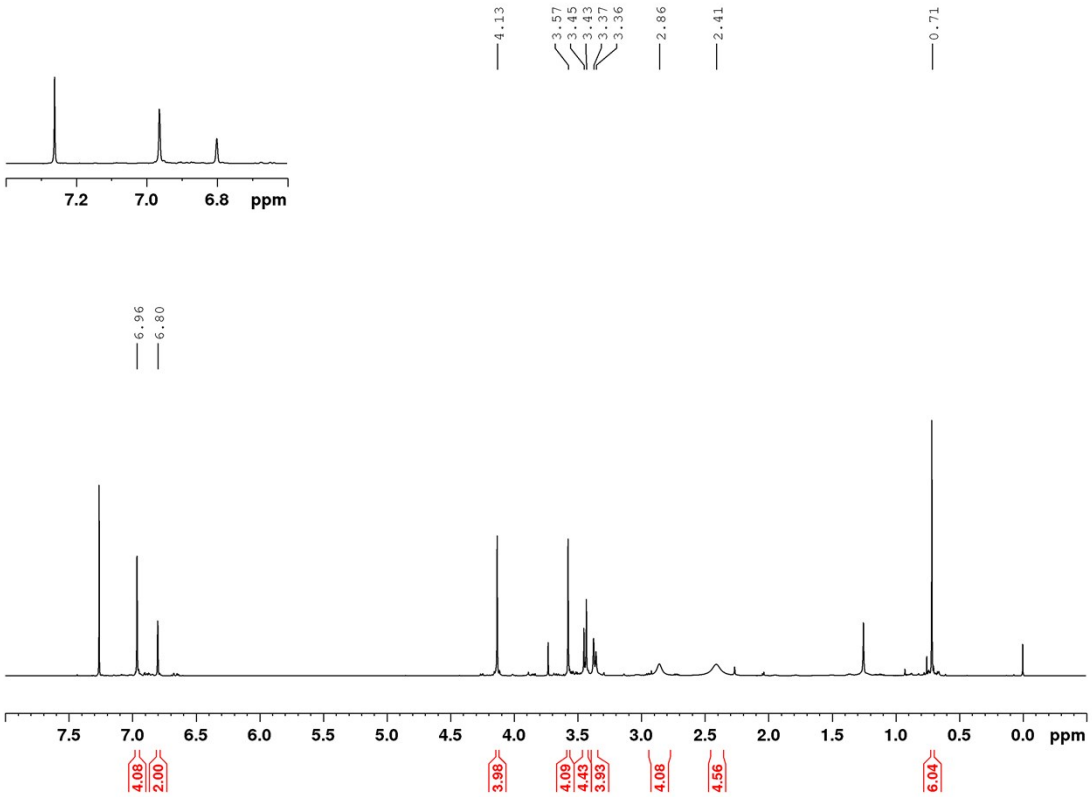

Fig. S 23: ^{1}H-NMR spectrum of compound **11** measured in deuterated chloroform at 300 K.

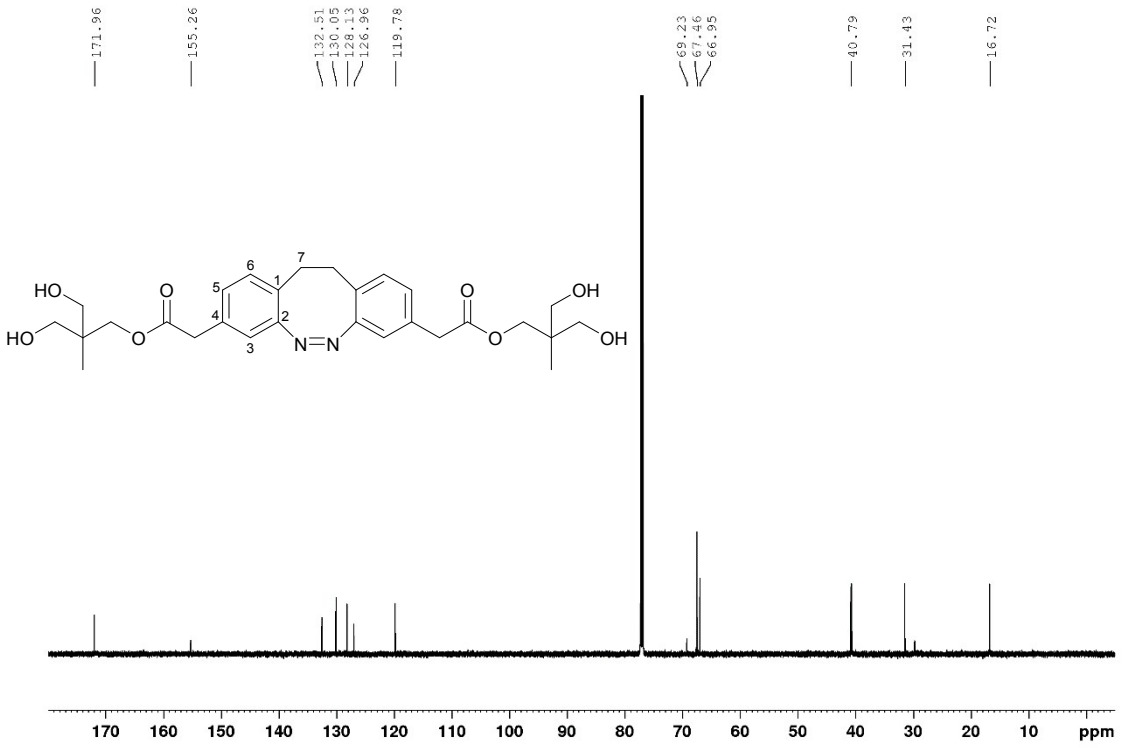

Fig. S 24: ^{13}C-NMR spectrum of compound **11** measured in chloroform at 300 K.

5.2.4.1. *Determination of the PSS of diazocine* 11

The PSS at 385 nm of diazocine **11** was determined in MeCN by integration of the *H*-3 signals of the *cis*- and the *trans*- isomer in the 1D-^{1}H-NMR spectrum of the PSS at 385 nm (**Fig. S 25**, red).

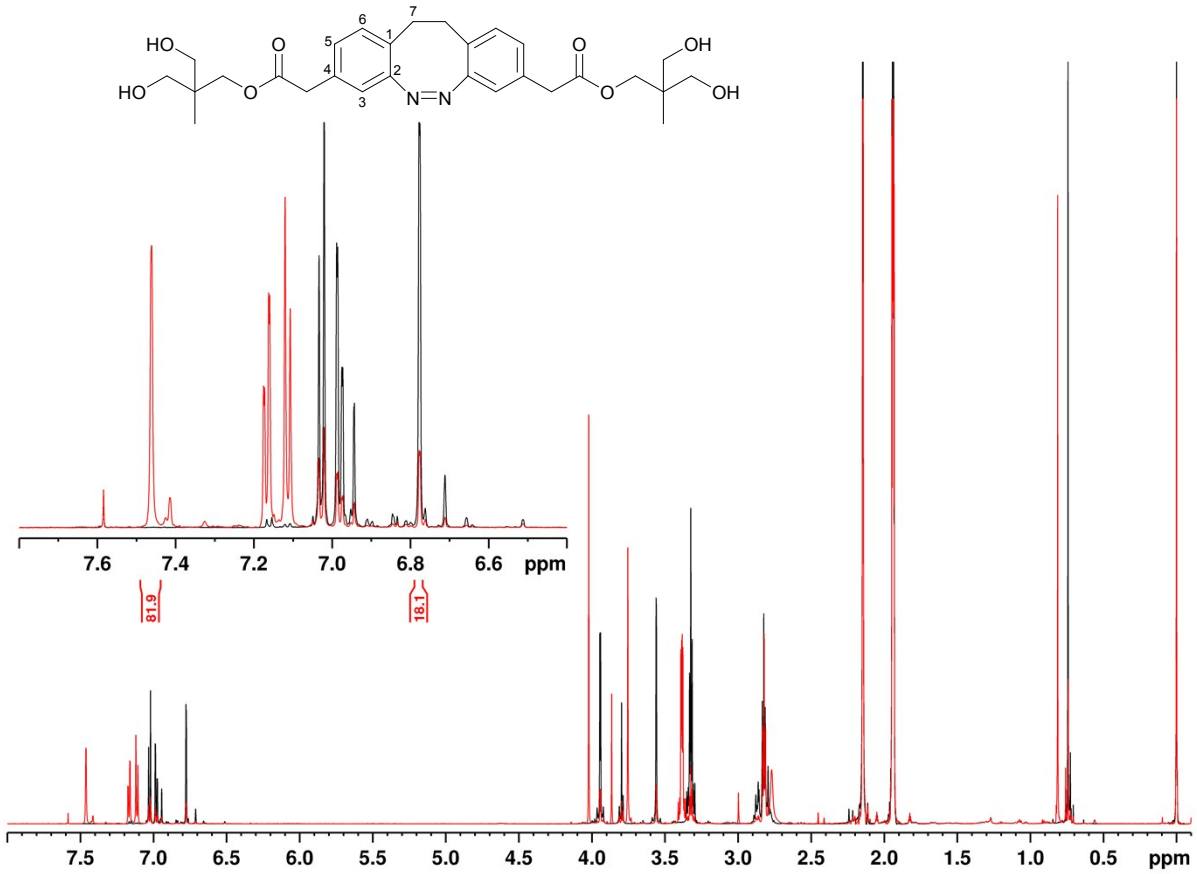

Fig. S 25: Overlay of the 1D-^{1}H-NMR spectra of diazocine **11** dissolved in MeCN-d_3. The spectrum displayed in black was recorded immediately after irradiation to the PSS at 530 nm, whereas the red spectrum represents the PSS at 385 nm. The expansion shows the aromatic region from which the PSS at 385 nm was determined by integration of the doublet at 7.46 ppm which represents the *trans*-species and at 6.78 ppm which represents the *cis*-isomer.

cis-diazocine 11 (black)

^{1}H-NMR (500.1 MHz, MeCN-d_3, 298 K): δ = 7.03 (d, ^3J = 7.9 Hz, 2 H, *H*-6), 6.98 (dd, ^3J = 7.9 Hz, ^4J = 1.6 Hz, 2 H, *H*-5), 6.79 (d, ^4J = 1.4 Hz, 2 H, *H*-3), 3.98-3.92 (m, 4 H, COO-CH_2-C), 3.56 (s, 4 H, COO-CH_2-C$_4$), 3.32 (m$_c$, 8 H, CH_2-OH, CH'_2-OH), 2.88-2.76 (m, 8 H, *H*-7, CH$_2$-O*H*), 0.74 (s, 6H, C-CH_3) ppm.

trans-diazocine 11 (red)

^{1}H-NMR (500.1 MHz, MeCN-d_3, 298 K): δ = 7.46 (s, 2 H, *H*-3), 7.17 (dd, ^3J = 7.8 Hz, ^4J = 1.6 Hz,2 H, *H*-5), 7.11 (d, ^3J = 7.8 Hz, 2 H, *H*-6), 4.02 (s, 4 H, COO-CH_2-C), 3.75 (s, 4 H, COO-CH_2-C$_4$), 3.38 (m$_c$, 8 H, CH_2-OH, CH'_2-OH), 2.86-2.72 (m, 8 H, *H*-7, CH$_2$-O*H*), 0.81 (s, 6H, C-CH_3) ppm.

5.2.5. Synthesis of (Z)-bis(2,5-dioxopyrrolidin-1-yl) 2,2'-(11,12-dihydrodibenzo[c,g][1,2]diazocine-3,8-diyl)diacetate (1)

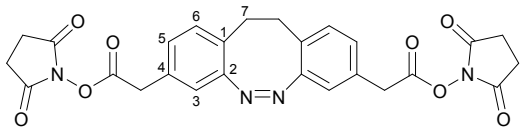

(Z)-bis(3-hydroxy-2-(hydroxymethyl)-2-methylpropyl) 2,2'-(11,12-dihydrodibenzo[c,g][1,2]diazocine-3,8-diyl)diacetate (**11**; 182 mg, 345 µmol) was dissolved in 5 ml MeOH/H_2O (4:1) and 5.5 ml 10% calcium carbonate solution was added. The reaction was stirred over night at room temperature. Afterwards the reaction was acidified to pH = 2 with 1 M hydrogen chloride solution and extracted with ethyl acetate (3 x 10 ml). The combined organic layers were washed with saturated sodium chloride solution, dried over magnesium sulfate and the solvent was evaporated in vacuo. Under N_2 atmosphere the crude product was dissolved in 5 ml DMF. 1-Ethyl-3-(3-dimethylaminopropyl)carbodiimide (EDC; 661 mg, 3.45 mmol) and *N*-hydroxysuccinimide (NHS; 199 mg, 1.73 mmol) were added at room temperature and the reaction stirred for 1 h. The reaction was added to 50 ml H_2O and extracted with (2 x 30 ml) DCM. The combined organic layers were washed with 10 % sodium bicarbonate solution, (2 x 50 ml) 0.1 M hydrogen chloride solution, 50 ml sodium chloride solution and dried over magnesium sulfate. The solvent was evaporated in vacuo and the crude product was purified by flash column chromatography (cyclohexane/ethyl acetate, 1:2) to afford the product as a yellow solid (45 mg, 87 µmol, 25%).

R_f: 0.43 (cyclohexane/ethyl acetate, 1:2)

T_m: 190 °C

^{1}H-NMR (500.1 MHz, DMSO-d_6, 300 K): δ = 7.12 (d, ^3J = 7.9 Hz, 2 H, *H*-6), 7.06 (dd, ^3J = 7.9 Hz, ^4J = 1.5 Hz 2 H, *H*-5), 6.89 (d, ^4J = 1.4 Hz, 2 H, *H*-3), 4.05 (s, 4 H, COO-CH_2-C_4), 2.82-2.81 (m, 12 H, *H*-7, CH_2-CH'_2) ppm.

^{13}C-NMR (125.8 MHz, DMSO-d_6, 300 K): δ = 170.0 (*C*O), 167.0 (*C*OO), 154.7 (*C*-2), 130.9 (*C*-1) 130.0 (*C*-6), 128.1 (*C*-5), 127 (*C*-4) 119.87 (*C*-3), 35.7 (COO-*C*H_2-C_4), 30.5 (*C*-7), 25.4 (*C*H_2-*C*'H_2) ppm.

IR (ATR): $\tilde{\nu}$ = 2925 (w), 1812 (w), 1781 (w), 1745 (s), 1727 (s), 1522 (w), 1497 (w), 1457 (w), 1426 (w), 1355 (m), 1205 (s), 1109 (m), 1062 (s), 991 (m), 963 (m), 892 (w), 877 (w), 846 (w), 807 (s), 758 (w), 738 (w), 646 (s) cm^{-1}.

HRMS (HR-ESI): $[C_{28}H_{36}O_8N_2 + NH_4]^+$, m/z = calc.: 536.1772, found 536.17759.

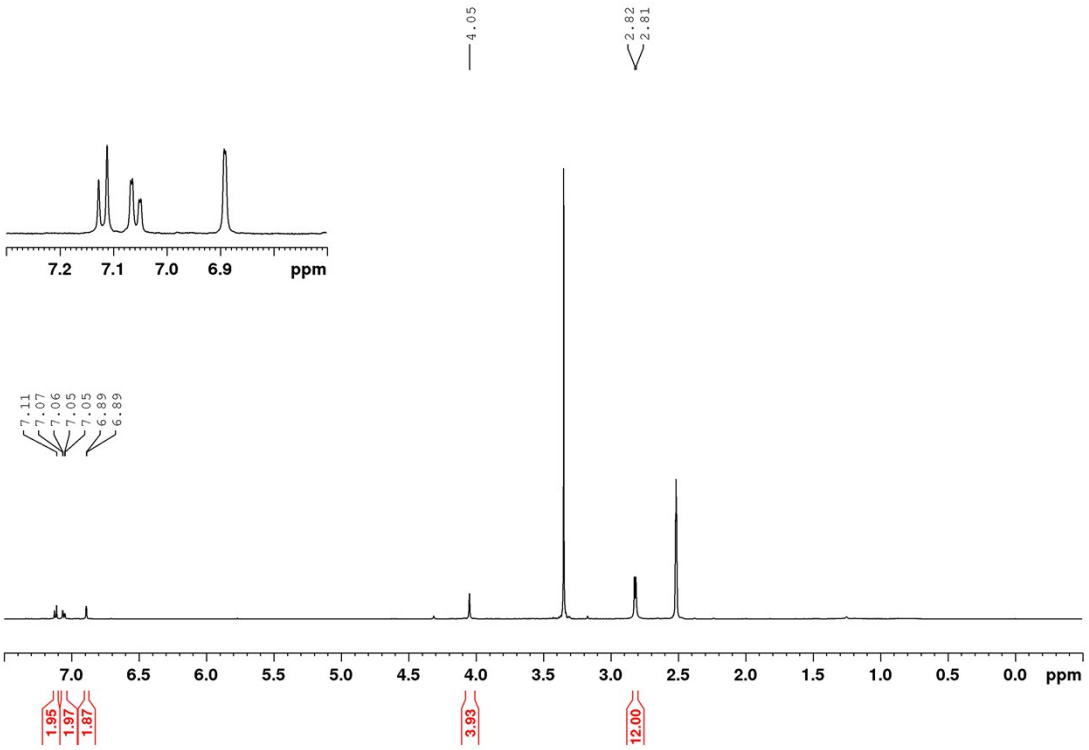

Fig. S 26: ^{1}H-NMR spectrum of compound **1** measured in deuterated DMSO at 300 K.

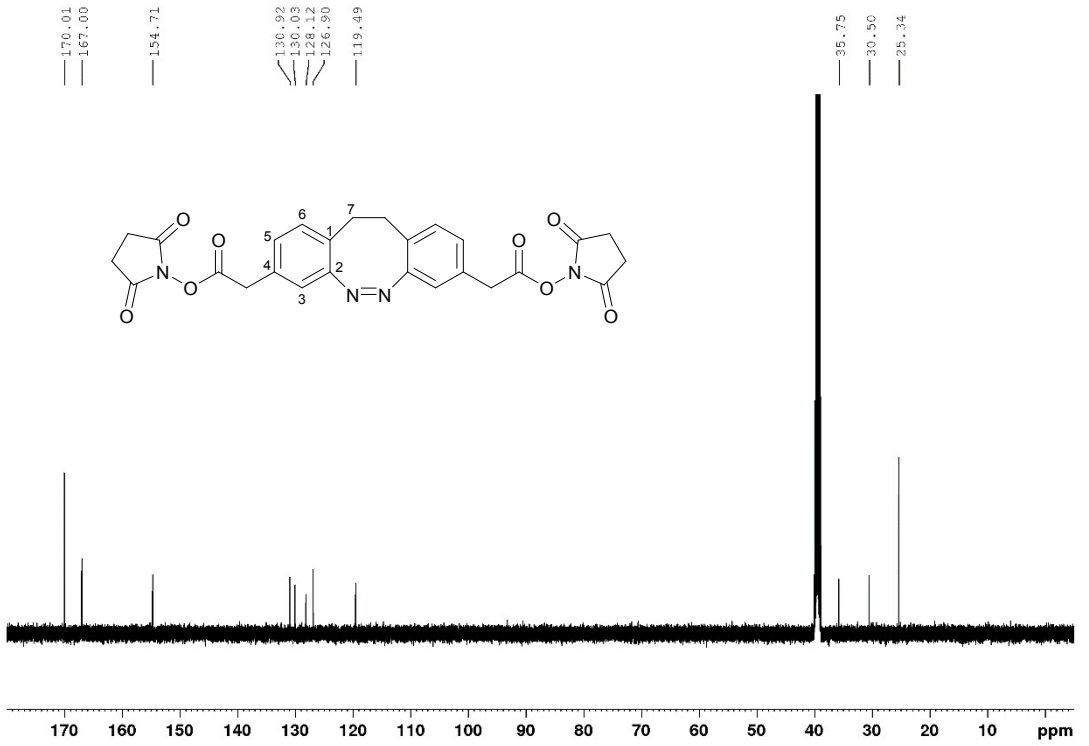

Fig. S 27: ^{13}C-NMR spectrum of compound **1** measured in deuterated DMSO at 300 K.

6. References

1. J. L. Markley, A. Bax, Y. Arata, C. W. Hilbers, R. Kaptein, B. D. Sykes, P. E. Wright and K. Wüthrich, *Pure and Applied Chemistry*, 1998, **70**(1), 117.
2. J. W. Neidigh, R. M. Fesinmeyer and N. H. Andersen, *Nat. Struct. Biol.*, 2002, **9**(6), 425.
3. B. Barua, J. C. Lin, V. D. Williams, P. Kummler, J. W. Neidigh and N. H. Andersen, *Protein Eng. Des. Sel.*, 2008, **21**(3), 171.
4. D. S. Wishart, C. G. Bigam, A. Holm, R. S. Hodges and B. D. Sykes, *J. Biomol. NMR*, 1995, **5**(1), 67.
5. A. Bundi and K. Wüthrich, *Biopolymers*, 1979, **18**(2), 285.